Model predictions of turbulent gas-particle shear flows

by

Tobias Strömgren

March 2010
Technical Reports from
Royal Institute of Technology
Department of Mechanics
SE-100 44 Stockholm, Sweden

Typsatt i $\mathcal{A}_{\mathcal{M}}\mathcal{S}\text{-}\mathbb{L}^{\!\!\!A}T_{\!\!\!E}\!X$

Akademisk avhandling som med tillstånd av Kungliga Tekniska Högskolan i Stockholm framlägges till offentlig granskning för avläggande av teknologie doktorsexamen måndagen den 29 mars 2010 kl 14.15 i sal F3 vid Kungliga Tekniska Högskolan, Lindstedtsvägen 26, Stockholm.

©Tobias Strömgren 2010 Universitetsservice US–AB, Stockholm 2010

Model predictions of turbulent gas-particle shear flows Tobias Strömgren

Linné Flow Centre Department of Mechanics, Royal Institute of Technology (KTH) SE-100 44 Stockholm, Sweden

Abstract

A turbulent two-phase flow model using kinetic theory of granular flows for the particle phase is developed and implmented in a finite element code. The model can be used for engineering applications. However, in this thesis it is used to investigate turbulent gas-particle flows through numerical simulations. The feedback from the particles on the turbulence and the mean flow of the gas in a vertical channel flow is studied. In particular, the influence of the particle response time, particle volume fraction and particle diameter on the preferential concentration of the particles near the walls, caused by the turbophoretic effect is explored. The study shows that when particle feedback is included the accumulation of particles near the walls decreases. It is also found that even at low volume fractions particles can have a significant impact on the turbulence and the mean flow of the gas.

The effect of particles on a developing turbulent vertical upward pipe flow is also studied. The development length is found to substantially increase compared to an unladen flow. To understand what governs the development length a simple estimation was derived, showing that it increases with decreasing particle diameters in accordance with the model simulations.

A model for the fluctuating particle velocity in turbulent gas-particle flow is derived using a set of stochastic differential equations taking into account particle-particle collisions. The model shows that the particle fluctuating velocity increases when particle-particle collisions become more important and that increasing particle response times reduces the fluctuating velocity. The model can also be used for an expansion of the deterministic model for the particle kinetic energy.

Descriptors: turbulent gas-particle flows, modelling, turbophoresis, two-way coupling, particle-particle collisions, numerical simulations

Preface

This thesis studies turbulent gas-particle shear flows. In the first part a short review of the basic concepts and methods is presented. The second part consists of the following papers:

Paper 1. Strömgren T., Brethouwer G., Amberg G. and Johansson A. V., 2009

"Modelling of turbulent gas-particle flows with focus on two-way coupling effects on turbophoresis", Submitted to Int. J. Multiphase Flow, 2009.

Paper 2. Strömgren T., Brethouwer G., Amberg G. and Johansson A. V., 2009

"A study of particle feedback in turbulent gas-particle flows", Proceedings of the $7^{\rm th}$ World Conference on Experimental Heat Transfer, Fluid Mechanics and Thermodynamics, 2009.

Paper 3. Strömgren T., Brethouwer G., Amberg G. and Johansson A. V., 2009

"A modelling study of evolving particle-laden turbulent pipe-flow", Submitted to Flow, Turbulence and Combustion, 2009.

Paper 4. Benavides A., Strömgren T., van Wachem B., Brethouwer G., Amberg G. and Johansson A. V., 2008

"Numerical computation of turbulent gas-particle flow in a backward-facing step. Model comparison with experimental data.", Proceedings of the 11th International Conference on Multiphase Flow in Industrial Plants, 2008.

Paper 5. Strömgren T., Brethouwer G., Amberg G. and Johansson A. V., 2010

"Modelling of particle fluctuations in turbulence by stochastic processes", Technical report, Linné Flow Centre, Dept. of Mechanics, KTH, Stockholm, Sweden

Parts of this work has been presented at:

Swedish Industrial Association for Multiphase Flows, Seminar May 10, 2007, Stockholm, Sweden

11th Nordic Pilot Center Meeting September 27-28, 2007, *Tampere, Finland*

$7^{\rm th}$ International Symposium on Engineering Turbulence Modelling and Measurements 1

June 4-6, 2008, Limassol, Cyprus

11th International Conference on Multiphase Flow in Industrial Plants² September 7-10, 2008, *Palermo*, *Italy*

EUROMECH Fluid Mechanics Conference 7

September 14-18, 2008, Manchester, UK

Svenska Mekanikdagarna

June 15-17, 2009, Södertälje, Sweden

$7^{\rm th}$ World Conference on Experimental Heat Transfer, Fluid Mechanics and Thermodynamics 3

June 28 - July 3, 2009, Krakow, Poland

$6^{\rm th}$ International Symposium on Turbulence, Heat and Mass Transfer 4

September 14-18, 2009, Rome, Italy

 $^{^1\}mathrm{With}$ written contribution to the conference proceedings: Strömgren T., Brethouwer G., Amberg G., Johansson A.V.: "Model simulations of two-way coupling effects on evolving particle-laden turbulent channel flows"

²With written contribution to the conference proceedings: Benavides A., Strömgren T., van Wachem B., Brethouwer G., Amberg G., Johansson A.V.: "Numerical computation of turbulent gas-particle flow in a backward-facing step. Model comparison with experimental data."

³With written contribution to the conference proceedings: Strömgren T., Brethouwer G., Amberg G., Johansson A.V.: "A study of particle feedback in turbulent gas-particle flows" ⁴With written contribution to the conference proceedings: Strömgren T., Brethouwer G., Amberg G., Johansson A.V.: "A modelling study of evolving particle-laden turbulent pipeflow"



Contents

Abstract	iii
Preface	iv
Chapter 1. Introduction	2
Chapter 2. Gas particle flows	4
2.1. Characteristics of turbulent gas-particle flows	4
2.2. Particle dynamics in turbulent flows	6
2.3. The influence of particles on the carrier phase	9
Chapter 3. Predicting gas-particle flows	11
3.1. Direct numerical simulations	11
3.2. Large eddy simulations	12
3.3. Closure models	12
3.4. Gas-particle model using kinetic theory of gra	anular flows 14
3.5. Other modelling approaches	18
Chapter 4. Numerical implementation	19
4.1. Automated code generation	19
4.2. Implementation into femLego	19
Chapter 5. Investigating gas-particle flows usi	ing models 22
5.1. Gas-particle flow in a channel and pipe	22
Outlook	29
Acknowledgements	31
Division of work between authors	33
Appendix A	35
A.1. Code report	35

Paper 1.	Modelling of turbulent gas-particle flows with focus on two-way coupling effects on turbophoresis	69
Paper 2.	A study of particle feedback in turbulent gas-particle flows	95
Paper 3.	A modelling study of evolving particle-laden turbulent pipe-flow	109
Paper 4.	Numerical computation of turbulent gas-particle flow in a backward-facing step. Model comparison with experimental data.	131
Paper 5.	Modelling of particle fluctuations in turbulence by stochastic processes	143

59

Bibliography

Part I Overview and summary

CHAPTER 1

Introduction

Examples of turbulent flows can be found everywhere in our daily life; the jet streams in the atmosphere, the wake behind a car, the flow in a waterfall and the smoke from a cigarette. One can see by observing these flows that their nature is very chaotic with a wide spectrum of scales in time and space. All these disparate flows are described by the Navier-Stokes equations derived by Navier and Stokes more than 150 years ago. However, due to the non-linearity of these equations a general solution does not exist for turbulent flows.

In a broad range of engineering applications and in nature turbulent flows carry particles. Examples of such flows are: sand storms; volcanic ash eruptions; dispersion of pollutants, pollen and allergens in air; micro-particle behaviour in smoke exhaust systems; fluidized bed combustion; food and pharmaceutical processing.

A turbulent flow laden with particles not only inherits all of the complexity from a single-phase flow but also has the complexity of the interaction between the particles and the gas phase. Single-phase flows can solely be characterised by the Reynolds number, i.e. the ratio between the inertial forces to viscous forces in the fluid. The characteristics of turbulent gas-particle flows are also dependent on particle concentration, size and density. Small particles will instantaneously follow even the smallest vortices of the flow while larger particles only partly will respond to the turbulent flow field. For low concentrations of particles the flow field is governed by the turbulence of the gas phase while for intermediate particle concentrations the particles have a substantial influence on the mean flow and the turbulence intensity of the gas phase. At high particle concentrations particle-particle collisions will govern the flow field.

Since the governing equations are known it is possible to numerically solve these equations exactly and use the solution to compute the particle path and also take into account the interaction between the particles and the gas phase. However, for large Reynolds numbers the required numerical resolution is very high. Even if computer resources have increased substantially the last years and will continue to do so only simpler problems can be studied. In order to investigate problems of engineering relevance turbulence models have to be used. Such models can only describe the mean flow while the turbulent fluctuations are modelled. Because of the coupling between the gas and the particle phase turbulent particle laden flows are very difficult to predict. As a consequence, modelling of turbulent particle-laden flows has historically not

been studied as much as single phase turbulent flow that is well established, thus being less mature. However, in order to develop industrial processes, optimise devices and forecast natural phenomena where gas-particle flows are present, it is of importance to have accurate models to describe and study these flows.

The present work is part of a long-term effort, with the aim to develop turbulent gas-particle models to investigate particle laden turbulent shear flows.

CHAPTER 2

Gas particle flows

2.1. Characteristics of turbulent gas-particle flows

A single phase flow is solely characterised by the Reynolds number, Re, i.e. the ratio between inertia forces to viscous forces

$$Re = \frac{Ul}{\nu} \tag{2.1}$$

where U, l and ν are a characteristic velocity, a characteristic length and viscosity, respectively. Compared to single phase flows gas-particle flows are more complex to characterise. Their behaviour is very dependent on the volume fraction of particles, Φ_p , and the Stokes number, St, which is the ratio between the particle response time, τ_p , to a characteristic flow time scale, τ_g , i.e.

$$St = \frac{\tau_p}{\tau_q} \tag{2.2}$$

where τ_p is the time it takes for a particle to reach 63% of the free stream velocity when released from rest (Crowe et al. 1998). If these parameters are known the strength of the interactions between the phases can be estimated.

Elghobashi (1994) constructed a map of regimes determining the interaction between particles and turbulence, which is shown in figure 2.1. Here τ_e is the turn over time for large eddies. For very small particle volume fractions, $\Phi_p < 10^{-6}$, the continuous phase is unaffected by the presence of particles. This is called one-way coupling because momentum is only transferred from the continuous phase to the particles. At higher Φ_p momentum will also be transferred from the particles to the continuous phase, implying two-way coupling. At even higher particle volume fractions ($\Phi_p > 10^{-3}$) particle-particle collisions will significantly contribute to the particle stress. This is called four-way coupling. In wall bounded flows particle-wall collisions will also be of importance for large Φ_p .

Hadinoto and Curtis (2004) divided gas-particle flows into three different regimes for increasing Φ_p : The macro-viscous regime where the transfer of momentum between gas and particles occur indirectly through the gas-phase, the transitional regime where the particle motion is affected by both particle-particle interactions and the gas phase viscosity and in the third, grain inertia regime, the particle motion is governed by particle-particle collisions.

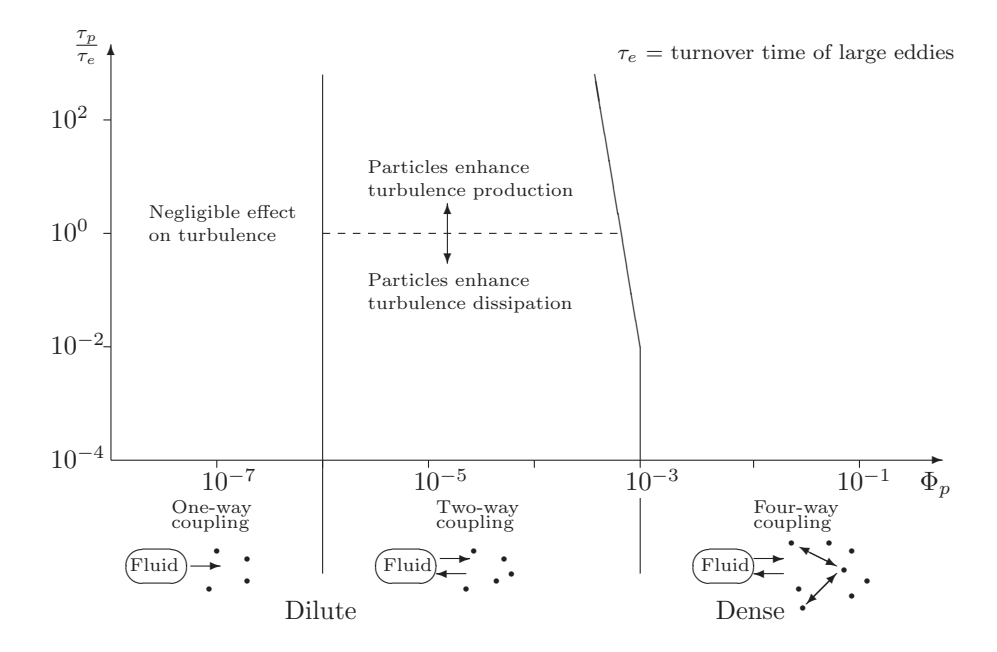


FIGURE 2.1. A sketch of the map of regimes of interaction between particles and turbulence from Elphobashi (1994).

Crowe et al. (1998) classified a particle laden flow as dilute if

$$\frac{\tau_p}{\tau_p^{col}} < 1 \tag{2.3}$$

where τ_p^{col} is the time between particle-particle collisions. In that case particles will have time to respond to the flow field of the gas phase between the collisions. If

$$\frac{\tau_p}{\tau_p^{col}} > 1 \tag{2.4}$$

a particle laden flow is regarded as dense because a particle will not have time to respond to the flow field between the collisions. Consequently, particle-particle collisions will govern the flow.

The particle response dependence on Stokes number is shown in figure 2.2. It is seen that the particles memory of its previous velocity increases with Stokes number (Squires & Eaton 1991). For St << 1 the response time of the particles is so small that they adjust instantaneously even to the smallest time scales of the flow and behave as passive scalars. In the other limit when St >> 1 the particle response time is very large compared to the time scale of the flow and

the particle is not affected by the flow. Particles with $St \sim 1$ respond to the larger time scales of the flow while they do not respond to the smaller time scales. In this regime it is known that in isotropic turbulence particles tend to concentrate in regions with low vorticity and high strain rate (Squires & Eaton 1991; Wood *et al.* 2005). Here the turbulent diffusion of the particles will be larger than that of the fluid because particles have smaller velocity fluctuations but larger autocorrelation time than the flow (Reeks 1977).

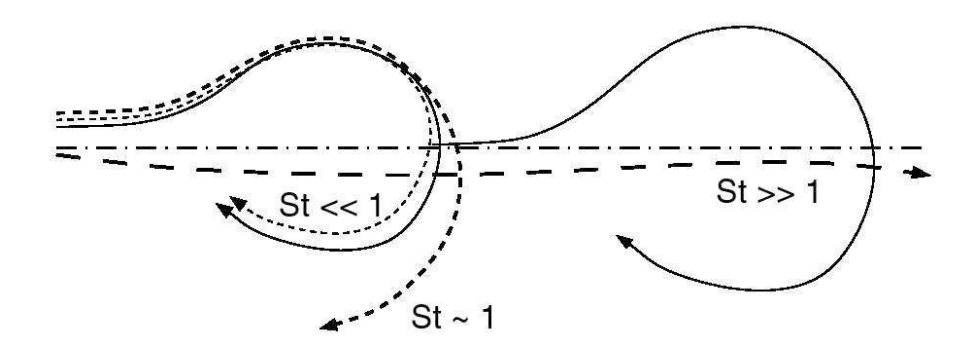


Figure 2.2. Effects of Stokes number on particle dispersion, from Crowe et al. (1998).

The "crossing trajectories effect" is when the particles have a mean relative velocity with respect to the gas flow (Reeks 1977; Squires & Eaton 1991). Gravity, for example can lead to particles crossing the turbulent vortices relatively fast. The consequences is that the vortices have only a short time to affect the particles leading to reduced turbulent particle dispersion (Wells & Stock 1983).

2.2. Particle dynamics in turbulent flows

2.2.1. Forces on a single particle

The motion of a single spherical particle in an unsteady flow at $Re_p \ll 1$ is described by the Basset-Boussinesq-Oseen (BBO) equation and has been derived by Maxey & Riley (1983). Here

$$Re_p = \frac{D_p |u_p - u_g|}{\nu_g} \tag{2.5}$$

is the particle Reynolds number, D_p is the particle diameter, u is the velocity and ν is the kinematic viscosity. Subscripts g and p are used to denote gas-and particle-phase, respectively. Here the BBO equation is presented without

the effects of a non-uniform flow

ects of a non-uniform flow
$$\frac{du_p}{dt} = \underbrace{\frac{\rho_g}{\rho_p} \frac{Du_g}{Dt}}_{Fluid\ acceleration} - \underbrace{\frac{1}{2} \frac{\rho_g}{\rho_p} \frac{d}{dt} (u_p - u_g)}_{Added\ mass} - \underbrace{\frac{1}{\tau_p} (u_p - u_g)}_{Stokes\ drag} + \underbrace{\frac{18}{4} \frac{\rho_g \nu_g}{D_p \rho_p} \int_{-\infty}^{t} \frac{\frac{d}{d\tau} (u_p - u_g)}{(\pi \nu_g (t - \tau))^{\frac{1}{2}}} d\tau}_{Basset\ force} + \underbrace{\frac{(1 - \frac{\rho_g}{\rho_p})g}{\rho_p}}_{Gravitational\ force} \tag{2.6}$$

where ρ is the density and g is the gravitational acceleration. The first term on the right hand side (R.H.S.) is the fluid acceleration term. The second term on the R.H.S. represents the force coming from the deceleration and acceleration of the surrounding fluid when a particle accelerates or decelerates, often called the added mass term. The difference in velocity between a particle and the surrounding fluid gives rise to viscous drag and pressure forces on the particle called Stokes drag, represented by the third term on the R.H.S. This is the force of the continuous phase on the particles which is the opposite to the added mass force. If $Re_p \sim O(1)$ or larger Stokes drag is not a good approximation and the term must be multiplied with a drag factor. Schiller & Naumann (1933) presented a drag factor f valid for particle Reynolds numbers up to 1000

$$f = 1 + 0.15Re_p^{0.687}. (2.7)$$

When a particle is accelerating or decelerating a force caused by the lagging of the boundary layer development acts on the particle. This term is called the Basset force or sometimes the history force and is represented by the fourth term on the R.H.S. There are only approximate models for the Basset force for small Re_p . The last term on the R.H.S. is the body force due to gravity.

In the present case, i.e. $\rho_p/\rho_g >> 1$, therefore the only terms that will have a significant contribution is the Stokes drag and the gravitational force (Sommerfeld et al. 2007).

Another force that could be of importance depending on the flow configuration is the lift force that a particle moving in a shear flow experiences due to the non-uniform pressure distribution around the particle. Saffman (1965) and Saffman (1968) derived an expression for the lift force which is only valid for low particle Reynolds numbers. Correction functions for higher Reynolds numbers have been derived but are not satisfactory (Sommerfeld et al. 2007). In a wall boundary layer this lift force is towards the wall if the particles are leading the flow and in the opposite direction if the particles lag the flow. Even though the lift force can be of importance in wall bounded flows (Young and Leeming 1997) it is not included in the present study since it does not change any of the main results of this study and adds more uncertainty in the modelling.

A rotating particle in a flow experiences a lift force, called Magnus force, caused by a pressure difference between the two sides of a particle due to the increased velocity on one side of the particle and a decreased velocity on the other side. Since particles can acquire high angular velocity after collisions with other particles or with a wall this effect can be of importance Sommerfeld (2003). However, it is not included in this study since particles with small diameters are considered ($< 100 \mu m$) where the Magnus force is relatively small (Lun & Liu 1997).

2.2.2. Preferential concentration of particles

Experiments and numerical simulations have shown that particles with $St \sim 1$ tend to have a mean convective drift in non-homogeneous turbulent flows as they move from regions with high turbulence intensity to regions with low turbulence intensity (see figure 2.2). The explanation is that particles are "thrown" from regions of high turbulence intensity to regions of lower turbulence intensity where there are no eddies with enough energy to disperse the particles back. This leads to a mean migration of particles counter to the fluctuating velocity gradient, which is often referred to as the effect of turbophoresis. In a channel or pipe flow particles with intermediate Stokes number accumulate in the viscous wall-layer close to the wall and possibly deposit on the walls (Fessler et al. 1994). This non-zero wall-normal mean particle velocity is counteracted by diffusion (Haarlem et al. 1998).

A model for particle transport and deposition to the wall was presented by Friedlander & Johnstone (1957). The distance where the drift towards the wall starts depends on the particle inertia and the intensity of the turbulent fluctuation velocity. Reeks (1983) described dispersion of discrete particles in a turbulent shear flow. In addition to the normal diffusion transport the effect of turbophoresis causes a flux proportional to the gradient of the local turbulence velocity correlation in a direction that transports particles from high to low turbulence intensities.

In order to study the physics of particle deposition in detail direct numerical simulations (DNS) were used by e.g. Rouson & Eaton (2001); Narayanan et al. (2003); Soldati & Marchioli (2009). Most of these studies assume flows with very small particle volume fractions so that the effects of particle feedback on the gas-phase and particle-particle collisions can be neglected. However, Li et al. (2001) studied the effects of turbophoresis for larger particle volume fractions taking into account the effects of two-way coupling while Nasr et al. (2009) also included particle-particle collisions in their DNS study. Experiments have been used as well to study preferential concentration of particles (see e.g. Wood et al. 2005; Fessler et al. 1994; Liu & Agarwal 1974). Models have also been used to study the effect of turbophoresis although they do not capture all of the physics (see e.g. Young and Leeming 1997; Shin et al. 2003; Slater et al. 2003). Most models used to study turbophoresis assume perfectly absorbing walls, i.e. particles are removed when they reach the wall (particle deposition). Cerbelli et al. (2001) assumed that particles are elastically reflected at the wall. In reality collisions are not totally elastic nor are all particles deposited at the wall, so a more realistic boundary condition should lie somewhere between these two.

2.3. The influence of particles on the carrier phase

2.3.1. Modification of the velocity profile

Tsuji et al. (1984) and Kulick et al. (1994) reported that in wall bounded turbulent gas-particle flows the profile of both particle- and gas phase velocity is more uniform than the single-phase velocity profile. The reason is that particles keep their high streamwise velocity as they drift from the core of the pipe to the wall because of their high inertia (Johansen 1991). The particle velocity at the wall is also non-zero while the gas has no-slip conditions there. Consequently, the particles have a higher velocity than the gas near the wall and thus increase the gas velocity through the drag force (Vreman 2007).

2.3.2. Turbulence modification

Particles can significantly affect turbulence depending on their size and density. Experiments have shown that small particles tend to attenuate turbulence while larger particles augment turbulence (Tsuji et al. 1984; Yarin & Hetsroni 1994; Kulick et al. 1994). Yuan & Michaelides (1992) listed three different mechanisms that contribute to turbulence modification of dilute gas-particle flows: dissipation of turbulent kinetic energy by the particles, shedding of vortices or the presence of wakes behind particles and fluid moving with the particle as added mass to the particle. Vortex shedding leads to turbulence enhancement while the dissipation effects leads to reduction. Achenbach (1974) showed experimentally that vortex shedding occurs for particles with $Re_p > 400$.

Gore & Crowe (1991) tried to identify the important parameters that control modification of turbulence intensity by analysing available data of pipe flows and showed that the ratio between particle diameter to turbulent length scale is the most important parameter to control the change of turbulent intensity due to particles. However, the magnitude of turbulence attenuation or enhancement was difficult to estimate since it will be affected by various parameters such as concentration, density ratio, flow Reynolds number and flow configuration (Hetsroni 1989). Vreman (2007) showed numerically that turbulence attenuation in wall-bounded flows decreases with mass loading for rather small mass loadings (<0.3). Tsuji et al. (1984) and Ljus et al. (2002) reported that for intermediate particle sizes the turbulence intensity was augmented in the centre of the pipe while it was damped in the near wall region.

2.3.3. Wall roughness and particle-particle collisions

The probability of particle-particle collisions mainly depends on particle volume fraction, diameter and fluctuating particle motion (Sommerfeld 2000). In dense flows the flow field will be governed by particle-particle collisions. But even in dilute flows (solid volume fraction $\sim 10^{-4}$) particle-particle collisions can affect the flow field (Vance et al. 2006; Li et al. 2001). Caraman et al. (2003) investigated the effect of collisions in a dilute pipe-flow and found that the radial fluctuation of particles was strongly influenced by particle-particle collisions

even for particle volume fractions as low as $5 \cdot 10^{-4}$. In the literature particle-particle collisions are modelled either following a deterministic (Tanaka & Tsuji 1991) or by a stochastic approach (Mitter *et al.* 2004). The deterministic approach is not suitable for large number of particles. In contrast, the stochastic approach can be used for large number of particles because it is computationally very efficient (Sommerfeld 2003).

Wall-roughness can have a strong effect on the particle fluctuating motion and affect the particle-wall collisions in wall-bounded flows. Sommerfeld (1992) developed a model for particle-wall collisions and found that it can have a large impact on the pressure loss, especially if the response time of the particles is so large that they do not have time to respond to the flow before they collide with the opposite wall. The lack of proper models for the wall roughness effects is one of the main reasons for discrepancies between simulation results and experiments (Vreman 2007).

CHAPTER 3

Predicting gas-particle flows

In order to predict gas particle flows numerical simulations are commonly used. The approaches can be divided into three main categories: Direct Numerical Simulations (DNS), Large Eddy Simulations (LES) and closure model simulations. Extensive reviews on modelling and simulation of turbulent dispersed two-phase flows can be found in Elghobashi (1994), Loth (2000) and Mashayek & Pandya (2003).

3.1. Direct numerical simulations

In DNS the governing equations are solved without using any models. All scales are resolved and all details of the flow are captured. However, DNS is computationally very expensive and only feasible for simple geometries and rather low Reynolds numbers. Therefore, it is not suitable for engineering applications, but DNS is very useful for getting a basic physical understanding of dispersed turbulent two-phase flows and can support the development of closure models. The particle phase is treated in a Lagrangian context, i.e. the particle phase is represented by a number of particles whose trajectories x_{pi} are computed by integrating:

$$\frac{dx_{pi}}{dt} = u_{pi} \tag{3.1}$$

and

$$\frac{du_{pi}}{dt} = \frac{1}{\tau_p} (u_{pi} - u_{gi}) \tag{3.2}$$

simultaneously. If the particle size is smaller than the smallest length scales of the flow, particles can be considered as 'point' particles, i.e. the flow around each particle is not resolved. Most DNS-studies do not take into account the feedback from the particles on the flow (one-way coupling). However, Vreman (2007), Li et al. (2001) and Mito and Hanratty (2006) have taken into account the feedback from the particles on the flow (two-way coupling). Nasr et al. (2009) also included particle-particle collisions (four-way coupling). Examples of DNS studies are Haarlem et al. (1998), Rouson & Eaton (2001), Narayanan et al. (2003) and Botto et al. (2005). Although computer resources have increased substantially the last years DNS is still too expensive to use for more complex geometries and flows with high particle concentrations and large Reynolds numbers.

3.2. Large eddy simulations

In LES the large scales are explicitly resolved, while the smaller scales are unresolved and accounted for by subgrid-scale (SGS) models. Thus LES can be used for higher Reynolds numbers and more complex geometries than DNS. In LES of turbulent particulate flows, the particle phase is mostly treated in a Lagrangian way. Examples of LES in the literature are Vance et al. (2006), Yamamoto et al. (2001) and Wang & Squires (1996). However, open issues still remain in the SGS modelling.

3.3. Closure models

In closure models the governing equations are averaged and modelled. This method is the least computationally demanding and can be used for engineering problems. However, due to the averaging unclosed terms appear that need to be modelled.

There are two approaches for modelling particles in gas-particle flows. In the Eulerian-Lagrangian approach each particle path is modelled while the gas phase is treated as a continuum. In the Eulerian-Eulerian (two-fluid) models both phases are treated as continua. The governing equations are averaged leading to unclosed terms that need to be modelled before the system can be solved. This method is the least computationally demanding and is suitable for engineering problems. The equations governing the two-fluid approach was derived from first principles by Anderson & Jackson (1967) and Ishii (1975).

Within two-fluid modelling there are two commonly used averaging methods: Reynolds averaging (non-weighted time averaging) and a volume fraction weighted averaging defined as

$$A_i = \frac{\langle a_i \Phi_k \rangle}{\langle \Phi_k \rangle} \tag{3.3}$$

where $<\cdot>$ indicates time- or ensemble-averaging and Φ_k is the volume fraction of phase k. Upper-case letter corresponds to averaged values and lower-case letters corresponds to instantaneous values. The volume fraction weighted average corresponds to the value of velocity and density that is obtained in experiments (Fan and Zhu 1998). The terms $<\phi'_k u'_{ki}>$ and $<\phi'_k u'_{ki}u'_{kj}>$ appearing in the momentum equation are non-zero when Reynolds averaging is used and lead to difficulties, but they are zero if volume fraction averaging is used. Here the prime implies the difference between the instantaneous and the averaged value of the variable, i.e. the fluctuating part. Since more unclosed terms will arise when using Reynolds averaging (Elghobashi & Abou-Arab 1983) the most common used approach is volume fraction averaging.

The difference between different two-fluid modelling approaches is mainly the treatment of the particle stresses (effective particle viscosity). The particle

stresses have contributions from the gas-phase turbulence and from particleparticle collisions. At high particle volume fractions stresses due to particleparticle collisions dominate. Whereas at low particle volume fractions particle stresses are mainly caused by turbulence.

There are three different approaches to treat the particle viscosity. The simplest approach is to treat the viscosity as constant throughout the fluid (Kuipers *et al.* 1992). However, in many flows the particle viscosity is nonuniform

A simple algebraic model where the particle viscosity is assumed to be a function of the turbulent gas phase viscosity was used by Elghobashi & Abou-Arab (1983), Pourahmadi & Humphrey (1983), Tu & Fletcher (1994), Young and Leeming (1997) and Strömgren et al. (2008). These models give good predictions for small Stokes numbers and dilute turbulent flows but for larger particle volume fractions they miss the important contribution of particle-particle collisions (Strömgren et al. 2009a).

The kinetic theory of granular flows uses an analogy to the kinetic theory of gases to derive balance equations for density, velocity and energy. The particles correspond to "amplified molecules" and Maxwellian velocity distribution for the particle velocity is assumed (Fan and Zhu 1998). The differences between molecular and granular equilibrium states are mainly due to gravity and inelastic collisions (Kanther et al. 2003). This approach gives an expression for particle viscosity containing contributions from both the turbulence and particle-particle collisions. Several models for kinetic theory of granular flows have been developed based on the work of Bagnold (1954) on the constitutive behaviour of rapid granular flows (Lun et al. 1984; Jenkins & Richman 1985; Sinclair & Jackson 1989; Louge et al. 1991; Bolio et al. 1995; Peirano & Leckner 1998; Zhang & Reese 2003; Lun & Savage 2003). Lun et al. (1984) were the first to describe the kinetic theory of granular flows and derived the constitutive relations for the solid phase. Jenkins & Richman (1985) later used Grad's 13-moment method and obtained a single particle velocity distribution function that could be used to integrate the collisional rate of change of any particle property. Louge et al. (1991) incorporated a one-equation turbulence model to combine the kinetic theory of dry granular flows with the gas phase turbulence. This was extended to a two-equation low-Reynolds number $K-\epsilon$ model by Bolio et al. (1995). Peirano & Leckner (1998) expanded the work of Jenkins & Richman (1985) to include effects of an interstitial gas, i.e. both the gas mean flow and fluctuational motion are taken into account and the gas phase turbulence will thus appear in the constitutive equations of the particle phase. This model is thus also suitable for dilute flows.

An advantage with models based on kinetic theory of granular flows compared to other models is that a constitutive relation of the particle stress is obtained. If the effects of the interstitial gas is taken into account the kinetic theory of granular flow models can be used for dilute flows, where they approach deterministic models (Balzer *et al.* 1996) and for dense flows where

particle-particle collisions dominate the flow. In kinetic theory of granular flows particle-particle collisions are assumed instantaneous and binary. However, this assumption is not valid for very dense flows where sustained contacts between particles occur. In that case an additional frictional stress will govern the flow and needs to be modelled (Zhang & Rauenzahn 1997).

A statistical approach where the governing equations are derived from the transport equation of the probability density function (pdf) of the particle velocity has been developed by Zaichik (1999), Fevrier *et al.* (2005) and Reeks (1991). One advantage with this approach is that the closure is in phase space and thus at a more basic level.

It is known that the anisotropy is larger in particle laden turbulence than in single-phase turbulence (Zhou 2010). Therefore there is a need for models that can handle such anisotropy better. Zhou & Chen (2001) derived a unified second-order moment two-phase turbulence model and solve the Reynolds stress transport equations. Taulbee et al. (1999) developed a Reynolds stress model which showed good agreement with DNS-data of a shear flow. Although, these models can handle more complicated flows the modelling is more difficult as there are more unclosed terms compared to isotropic closures.

3.4. Gas-particle model using kinetic theory of granular flows

Below a turbulent gas-particle model based on the kinetic theory of granular flows is shown. This model is used in this thesis and is mainly based on the work of Balzer *et al.* (1996), Peirano & Leckner (1998), Zhang & Reese (2003) and Benavides & van Wachem (2008).

3.4.1. Conservation equations

The volume fraction averaged mass and momentum equations read

$$\frac{\partial}{\partial t}(\Phi_k \rho_k) + \frac{\partial}{\partial x_i}(\Phi_k \rho_k U_{kj}) = 0 \tag{3.4}$$

$$\frac{\partial}{\partial t}(\Phi_k \rho_k U_{ki}) + \frac{\partial}{\partial x_j}(\Phi_k \rho_k U_{ki} U_{kj}) = -\frac{\partial}{\partial x_j}(\Phi_k P_g)
+ \frac{\partial}{\partial x_j} \Pi_{k,ij} + f_{k,i} + \Phi_k \rho_k g_i$$
(3.5)

where ρ is the density, U is the mean velocity, Π is the stress tensor, P_g is the gas phase pressure and f_i is the drag term representing the inter phase momentum exchange. Only the drag force and the gravitational force are included since we only consider flows with $\rho_p/\rho_g >> 1$. Global continuity implies that $\Phi_g + \Phi_p = 1$. The averaging volume is much smaller than the characteristic length scale of the flow and much larger than the particles. For a complete derivation of the instantaneous equations governing two phase flow see for example Anderson & Jackson (1967) and Enwald $et\ al.\ (1996)$.

3.4.2. Inter phase momentum exchange

The drag force acting on a particle in a flow field through form drag is the dominating force in most gas flows laden with heavy particles. If particle volume fraction is larger than 10^{-5} (Strömgren et al. 2009a) also the gas phase will be affected by the particles through the drag, i.e. two-way coupling. This momentum exchange between the phases is commonly modelled as (Crowe et al. 1998)

$$f_{p,i} = -f_{g,i} = \Phi_p \rho_p \frac{U_{r,i}}{\tau_{pg}^f}$$
 (3.6)

where

$$\tau_{pg}^f = \frac{24\tau_p}{C_D Re_r} \tag{3.7}$$

is the characteristic time scale of gas-particle momentum transfer. $C_D = \frac{24}{Re_r} (1 + 0.15 Re_r^{0.687})$ is the drag coefficient valid for $Re_r < 1000$ (Schiller & Naumann 1933).

$$Re_r = \frac{|u_r|D_p}{\nu_q} \tag{3.8}$$

is the relative Reynolds number and

$$\tau_p = \frac{\rho_p D_p^2}{18\rho_q \nu_q} \tag{3.9}$$

is the particle response time. The mean relative velocity is written as $U_{r,i} = (U_{p,i} - U_{g,i}) - U_{d,i}$ where $U_{d,i}$ is the average of the fluid velocity fluctuations with respect to the particle distribution (Simonin *et al.* 1993; Benavides 2008), and is modelled according to

$$U_{d,i} = \frac{1}{3} K_{pg} \tau_{pg}^t \left(\frac{1}{\Phi_p} \frac{\partial \Phi_p}{\partial x_i} - \frac{1}{\Phi_g} \frac{\partial \Phi_g}{\partial x_i} \right)$$
 (3.10)

where $K_{pg} = \overline{u'_{p,i}u'_{g,i}} \approx \sqrt{2K_g3T}$ (Hadinoto and Curtis 2004) is the gas-particle fluctuating velocity correlation. For a comparison between different models for K_{pg} see Benavides & van Wachem (2008). $K_g = \frac{1}{2}\overline{u'_{gi}u'_{gi}}$ is the mean kinetic energy and $T = \frac{1}{3}\overline{u'_{pi}u'_{pi}}$ is the granular temperature, or particle kinetic energy.

$$\tau_{pq}^t = \tau_q^t (1 + C\xi)^{-1/2} \tag{3.11}$$

is the correlation time scale of the gas phase turbulence viewed by the particles and

$$C = 1.8 - 1.35 \left(\frac{U_{r,i} U_{p,i}}{|U_{r,i}| |U_{p,i}|} \right)^2, \tag{3.12}$$

$$\xi = \frac{3|U_{r,i}|^2}{2K_g} \tag{3.13}$$

and

$$\tau_g^t = \frac{3}{2\omega} \tag{3.14}$$

(Thai Van et al. 1994) is the Eulerian time scale of the gas phase turbulence and ω is the inverse time scale of the gas phase turbulence.

The absolute value of the instantaneous relative velocity is modelled as (Benavides & van Wachem 2008; Balzer et al. 1996)

$$|u_r| = \sqrt{U_{r,i}U_{r,i} + \overline{u'_{r,i}u'_{r,i}}} = \sqrt{U_{r,i}U_{r,i} + 2/3(K_g - K_{pg}) + T}.$$
 (3.15)

3.4.3. Particle phase stress

In a turbulent gas-particle flow the particulate stress has contributions from both particle-particle collisions and gas phase turbulence. Both contributions are considered within the kinetic theory approach taking the interstitial fluid into account (Peirano & Leckner 1998; Balzer *et al.* 1996; Zhang & Reese 2003). The particle stress is then expressed as

$$\Pi_{p,ij} = \left(P_p - \lambda_p \frac{\partial U_{p,m}}{\partial x_m}\right) \delta_{ij} - \left(\nu_p^{col} + \nu_p^{kin}\right) \left(S_{p,ij} - \frac{2}{3} \frac{\partial U_{p,m}}{\partial x_m}\right)$$
(3.16)

where

16

$$P_p = \Phi_p \rho_p T \left(1 + 2\Phi_p g_0 (1 + e_p) \right) \tag{3.17}$$

is the granular pressure,

$$\nu_p^{col} = \frac{4}{5} \Phi_p g_0 (1 + e_p) \left(\nu_p^{kin} + D_p \sqrt{\frac{T}{3\pi}} \right)$$
 (3.18)

is the collisional viscosity and

$$\nu_p^{kin} = \frac{2}{3} \left(K_{pg} \frac{\tau_{pg}^t}{\tau_{pg}^f} + T(1 + \zeta_c \Phi_p g_0) \right) \left(\frac{2}{\tau_{pg}^f} + \frac{\sigma_c}{\tau_p^{col}} \right)^{-1}$$
(3.19)

is the kinematic viscosity. In the limit of small Stokes numbers and small particle volume fractions ν_p^{kin} approaches the turbulent viscosity of the gas phase. $\lambda_p = \frac{5}{3} \rho_p \Phi_p \nu_p^{col}$,

$$g_0 = \frac{1}{1 + \sqrt{\frac{\Phi_p}{\Phi_{p,max}}}} \tag{3.20}$$

is the pair correlation function where $\Phi_{p,max}=0.64$, $S_{k,ij}=\frac{1}{2}(\frac{\partial U_{k,i}}{\partial x_j}+\frac{\partial U_{k,j}}{\partial x_i})$ is the mean strain rate tensor, e_p is the coefficient of restitution, $\zeta_c=\frac{2}{5}(1+e_p)(3e_p-1)$, $\sigma_c=\frac{1}{5}(1+e_p)(3-e_p)$ and

$$\tau_p^{col} = \frac{D_p}{24\Phi_p g_0} (\frac{\pi}{T})^{1/2} \tag{3.21}$$

is the inter particle collisional time scale.

The equation for granular temperature, T, can be derived in a similar way as K_q . In order to close the unclosed correlations the kinetic approach is used

$$\frac{3}{2}\rho_p\Phi_p\frac{\partial T}{\partial t} + \frac{3}{2}\rho_p\Phi_pU_{p,j}\frac{\partial T}{\partial x_j} = 2\rho_p\Phi_p(\nu_p^{col} + \nu_p^{kin})S_{p,ij}S_{p,ij} - \rho_p\Phi_p\frac{(1 - e_p^2)}{2\tau_p^{col}}T + \frac{\partial}{\partial x_j}\left\{\frac{3}{2}\rho_p\Phi_p(\kappa_p^{kin} + \kappa_p^{col})\frac{\partial T}{\partial x_j}\right\} + (1 + 0.15Re_r^{0.687})\frac{\rho_p\Phi}{\tau_p}(K_{pg} - 3T)$$
(3.22)

where

$$\kappa_p^{col} = \Phi_p g_0 \left(1 + e_p \right) \left(\frac{6}{5} \kappa_p^{kin} + \frac{4}{3} D_p \left(T/\pi \right)^{1/2} \right)$$
 (3.23)

is the collisional contribution to the diffusivity

$$\kappa_p^{kin} = \left(\frac{3}{5} \frac{\tau_{pg}^t}{\tau_{pg}^f} K_{pg} + T \left(1 + \Phi_p g_0 \frac{3}{5} (1 + e_p)^2 (2e_p - 1)\right)\right) \left(\frac{9}{5\tau_{pg}^f} + \frac{\xi_p}{\tau_p^{col}}\right)^{-1} (3.24)$$

is the kinetic contribution to the diffusivity and $\xi_p = \frac{1}{100}(1+e_p)(49-33e_p)$. The last term in equation (3.22) represents the interaction between the particle phase and the gas phase.

The wall-boundary conditions used for U_p and T are those originally developed by Johnson & Jackson (1987) for granular flows:

$$\left(\nu_p^{col} + \nu_p^{kin}\right) \frac{\partial U_p}{\partial y} = -\frac{\pi g_0 \varphi U_p \sqrt{3T}}{6\Phi_p^{max}}$$
(3.25)

$$\left(\kappa_p^{col} + \kappa_p^{kin}\right) \frac{\partial T}{\partial y} = \frac{\pi g_0 \varphi U_p^2 \sqrt{3T}}{6\Phi_p^{max}} - \frac{\pi g_0 (1 - e_w^2)(3T)^{3/2}}{12\Phi_p^{max}}$$
(3.26)

where φ is the specularity coefficient describing the wall roughness and e_w is the coefficient of particle wall restitution.

The stress term for the gas phase using the Boussinesq approximation for the Reynolds stress reads

$$\Pi_{g,ij} = \rho_g \left(\Phi_g \left(2(\nu_g + \nu_{tg}) S_{g,ij} - \frac{2}{3} \delta_{ij} \left(K_g + \nu_{tg} \frac{\partial U_{g,l}}{\partial x_l} \right) \right) \right). \tag{3.27}$$

In order to model ν_{tg} two-equation turbulence models such as, $K_g - \epsilon$ or $K_g - \omega$ are most commonly used (Strömgren et al. 2009a; Benavides & van Wachem 2008; Chan et al. 2005; Benyahia et al. 2007) whereby the Boussinesq assumption is used in order to model ν_{tg} . In the K_g , ω and ϵ equations an extra term is included to take into account the interaction between the gas phase and the particle phase arising from the Stokes drag.

A shortcoming of the Boussinesq assumption is the poor description of strongly anisotropic turbulence. Reynolds stress transport models solving transport equations for the Reynolds stresses are better suited to model strongly anisotropic turbulence. An intermediate type of model is the Explicit Algebraic Reynolds Stress Model (EARSM) that uses an explicit relation between the Reynolds stress anisotropy and the mean strain and rotation rate tensors. This kind of model can capture the physics in strongly anisotropic turbulence by only solving two transport equations for the turbulence quantities (two-equation models) (Wallin and Johansson 2000). Reeks (1993) used a kinetic approach to evaluate the Reynolds stresses and compared it with the Boussinesq assumption and found that the kinetic approach was better for anisotropic turbulence.

3.5. Other modelling approaches

18

In very dilute gas particle flows with small Stokes numbers particle-particle collisions do not give any contribution to the stress and a more simplified deterministic model for the particulate stress can be used without loss of accuracy (Strömgren et al. 2009a; Arcen et al. 2008). In this parameter range both the particle kinetic energy and the particulate stress can be describe analogously as the gas phase. A simple model originally derived by Hinze (1959) can be used, i.e.

$$K_p = \frac{K_g}{1 + \frac{\tau_p}{T_L}} \tag{3.28}$$

where T_L is the Lagrangian time scale. The particle stress is described as $2\nu_{pt}S_{p,ij}$ where

$$\nu_{tp} = \frac{\nu_{tg}}{1 + \frac{\tau_p}{T_L}} \tag{3.29}$$

(Melville & Bray 1979) where ν_{tg} is the turbulent viscosity of the gas phase. This modelling approach has been used by for example Tu & Fletcher (1994), Young and Leeming (1997) and Strömgren et al. (2009b). In this case the particle viscosity and kinetic energy are assumed to be governed by the gas phase turbulence. Therefore, this approach is only valid for small particle volume fractions and small particles. To improve predictions a similar two-equation model to that for the gas phase can be used for the particle phase. Wang et al. (1997) developed a $K_g - \epsilon - K_p - \epsilon_p$ model with similar mean turbulent kinetic energy and energy dissipation transport equations for the particle phase and the gas phase.

CHAPTER 4

Numerical implementation

4.1. Automated code generation

In order to solve the turbulent gas-particle models used in this study a finite element based automated code generator, femLego, is used (Amberg et al. 1999; Do-Quang et al. 2007). An advantage with using femLego is that the system of equations are specified in a general format since femLego uses symbolic computation in Maple coupled with automated code generation. Since the derivation is done by femLego more effort can be put into the physics and understanding of the equations. This makes femLego a very good tool for developing models.

The numerical scheme used in this study is based on a projection method for incompressible Navier-Stokes (Guermond & Quartapelle 1997) where a sequence of decoupled equations for velocity and pressure is solved at each time step.

The femLego toolbox generates a finite element code in C & C++. Triangular elements are used and both linear and quadratic test functions can be used. The code is highly parallelised and inherits adaptive mesh refinement capabilities.

4.2. Implementation into femLego

In order to solve a system of equations with femLego the equations are written on a weak form, i.e. multiplied with a test function and integrated over the volume, in a Maple worksheet together with boundary conditions, initial conditions and the method used to solve the resulting matrix of each equation. The equations are formulated in tensor form using the femLego syntax. The nabla operator $\frac{\partial}{\partial x_j}$ is implemented as $\mathtt{nab}(\ldots)[j]$ and &t between tensors invoke the Einstein summation rule.

4.2.1. A simple example

Below a simple example is given on how the heat equation is written on a weak form and implemented into femLego. The heat equation reads

$$\frac{\partial T}{\partial t} = \kappa \frac{\partial^2 T}{\partial x_i^2} \tag{4.1}$$

where T is the temperature and κ is the thermal diffusivity. In order to write equation (4.1) on a weak form it is multiplied with a test function, η , and integrated over a volume, i.e.

$$\int \eta \frac{\partial T}{\partial t} dV = \int \eta \kappa \frac{\partial^2 T}{\partial x_i^2} dV. \tag{4.2}$$

Since only linear test functions are used in the present study second order derivatives cannot be resolved. Therefore, all second order derivatives must be partially integrated in order to only have first order derivatives. Doing this equation (4.2) becomes

$$\int_{\Omega} \eta \frac{\partial T}{\partial t} dV = -\int_{\Omega} \kappa \frac{\partial \eta}{\partial x_i} \frac{\partial T}{\partial x_i} dV + \int_{\Omega} \frac{\partial}{\partial x_i} \left(\kappa \eta \frac{\partial T}{\partial x_i} \right) dV. \tag{4.3}$$

Using Gauss theorem the last term can be written as a surface integral. The problem can now be expressed as: Find a function $T \in V$ so that

$$\int_{\Omega} \eta \frac{\partial T}{\partial t} dV = -\int_{\Omega} \kappa \frac{\partial \eta}{\partial x_i} \frac{\partial T}{\partial x_i} dV + \int_{\Gamma} \kappa \eta \frac{\partial T}{\partial n} dS \qquad \eta \in V$$
 (4.4)

for all η , where Ω is an enclosed volume with the boundary Γ and V is all suitable functions. After discretising in time the equation in femLego syntax looks like

ElementInt(eta(x,y)*(T(x,y)-TO(x,y))/dt) =

-ElementInt(kappa*nab(eta(x,y))[i] &t nab(T(x,y))[i])

+BoundaryInt(eta(
$$x,y$$
)*BoundaryValue*qBCval) (4.5)

where ElementInt(...) is volume integration, BoundaryInt(...) is surface integration, BoundaryValue * qBCval = $\frac{\partial T}{\partial n}$ is the value of T at the boundary and qBCval is a predefined name in femLego that is used as a boundary value parameter which is specified with the mesh. Boundary conditions and initial conditions are specified in the Maple script.

Different numerical solvers can be used to solve the linear system of algebraic equations that each equation gives rise to. For stiff matrices direct methods are preferred. The asymmetric multi-frontal method (UMFPACK) provides fast and accurate direct solvers (Davis 2004). However, iterative methods are more efficient such as the conjugate gradient method (CG) that only can be used for symmetric matrices. For asymmetric matrices the generalised minimum residual method (GMRES) can be used. For simple relations, i.e. without any derivatives, CopyEq(...) can be used instead of ElementInt(...) for volume integration.

When the Maple script is compiled a C++ code is automatically generated which is compiled and an executable file for the problem is created. Size of the time step, parameters etc. are specified in an indata file.

4.2.2. Implementation of turbulent particle laden models

The model presented in section 3.4 is implemented in cylindrical coordinates into femLego. The two-dimensional pipe geometry was axisymmetric and was

constructed with uniform spacing in streamwise direction and refined spacing close to the wall in the radial direction. A low Reynolds number $K_g - \omega$ model is used for the gas phase turbulence.

Boundary conditions for both gas- and particle velocities and kinetic energy has a Dirichlet condition at the inlet and a Neumann condition at the outlet. The pressure has a Dirichlet condition at the outlet and a Neumann condition at the inlet. The gas phase velocity and kinetic energy has a no-slip condition at the wall. Wall boundary conditions for the particle velocity and granular temperature are those specified in equation (3.25) and (3.26) in section 3.4.3.

The accumulation of particles in the near wall region in wall bounded shear flows, described in section 2.2.2, causes a slightly larger pressure in that region. The wall-normal pressure distribution will therefore be non-homogeneous. In order to have a numerically stable boundary condition at the outlet the following condition is given

$$P|_{outlet} = -\frac{2}{3}K_g. (4.6)$$

The inverse time scale of the turbulence ω has the following near wall behaviour

$$\omega_w = \frac{6\nu}{\beta y^2} \tag{4.7}$$

where ν is the gas kinematic viscosity, β is a constant and y is the wall distance. This causes numerical difficulties in the near-wall region since $\omega \to \infty$ as $y \to 0$. In order to capture the rapid growth of ω in the near wall-region a decomposition was introduced, $\omega = \tilde{\omega} + \omega_w$ (Gullman-Strand *et al.* 2004). An equation is solved for $\tilde{\omega}$ which is zero at the wall. ω_w is chosen according to (4.7).

For the transport equations of momentum and kinetic energy GMRES is used as solver while CG is used for the pressure and the particle volume fraction. fem-Lego does not provide any post-processing but output can be processed in most programs. In this work foremost Matlab has been used for post-processing.

The turbulent gas-particle model based on kinetic theory of granular flows, presented in section 3.4, implemented in cylindrical coordinates into femLego is printed in appendix A.

CHAPTER 5

Investigating gas-particle flows using models

Developing closure models for turbulent particle-laden flows is a rather young research area due to complex physics. The aim of this thesis is to develop tools to study turbulent gas-particle flows in engineering problems. Investigation of such models is of great importance since they contribute to the design and optimisation of many industrial processes. A two fluid approach was chosen and different versions of the model presented in section 3.4 were implemented into a finite element code, femLego (Do-Quang et al. 2007).

5.1. Gas-particle flow in a channel and pipe

5.1.1. The importance of two-way coupling

Usually it is assumed that in very dilute gas-particle flows the momentum transfer from the particles to the gas phase is negligible. The effect of two-way coupling on relatively dilute flows in an upward vertical channel flow was investigated in paper 1. Simulation results for different mass loadings were compared between a model including two-way coupling and a model with only one-way coupling. It is shown that in relatively dilute flows the momentum transfer from the particles on the gas phase (two-way coupling) can have a crucial impact on the flow field.

Figure 5.1 shows the difference between the gas velocity, U_g , obtained from a simulation with one-way coupling and simulations with two-way coupling for three different mass loadings. The pressure gradient was the same in all simulations. The profiles are normalised with the maximum value of U_g for one-way coupling. For $\Phi_p = 1 \cdot 10^{-5}$ the effect of two-way coupling is negligible, but when $\Phi_p = 5 \cdot 10^{-5}$ the difference between one- and two-way simulations are about 10%. When $\Phi_p = 2 \cdot 10^{-4}$ the differences are substantial. The centreline velocity in the simulation with two-way coupling is 50% lower than in the simulation with one-way coupling.

5.1.2. The influence of turbophoresis on the particle distribution

The accumulation of particles in a turbulent flow in regions with low turbulence intensity due to the effect of turbophoresis is a well known phenomena. In wall bounded shear flows, as pipe- or channel flows, this effect causes particles within a certain parameter range to accumulate in the near wall region. The drift of particles to the near wall region is caused by the gradient of K_q . The influence

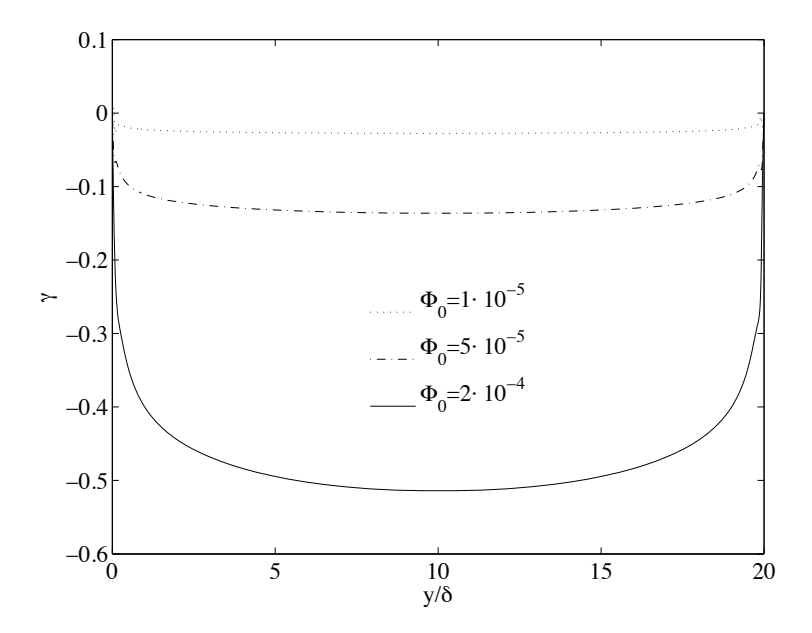


FIGURE 5.1. Difference between mean gas velocities obtained from simulations with one- and two-way coupling normalised with maximum mean gas velocity for one-way coupling, $\gamma = \frac{U_{g,2W}-U_{g,1W}}{max(U_{g,1W})}$, $\rho_p = 910 \, kg/m^3$ and $D_p = 40 \mu m$.

of particle diameter on the turbophoretic effect was studied in both paper 1 and 2. In figure 5.2 the particle volume fraction, Φ_p , normalised with its initial value, $\Phi_0 = 2 \cdot 10^{-4}$, is shown for 6 different particle diameters, D_p , for a fully developed channel flow. Close to the wall the particle volume fraction is more than hundred times larger than in the core region. The turbophoretic effect becomes stronger with D_p up to 40 μm but diminishes for large particles. This non-monotonic behaviour is expected since for very small D_p , i.e. small particle response times, the particles respond even to the smallest turbulent length scales and for large D_p , i.e. large particle response times, the particles will not respond to the turbulence. This implies that the turbophoretic effect vanishes for large and small D_p . The turbophoretic effect will therefore have its largest impact when particles respond to the turbulence but do not perfectly follow the flow.

The maximum value of Φ_p/Φ_0 is found at the wall and is shown as a function of τ_p^+ in figure 5.3 for four different Reynolds numbers. τ_p^+ is the particle response time normalised by the viscous time scale ν_g/u_τ^2 for the different cases. Φ_p/Φ_0 reaches a maximum for $\tau_p^+=13$ for all Reynolds numbers except for Re=10 000 where the maximum occurs at $\tau_p^+=9$. The particle volume fraction close to the wall increases for increasing Reynolds numbers due to the increased gradient of the turbulent intensity.

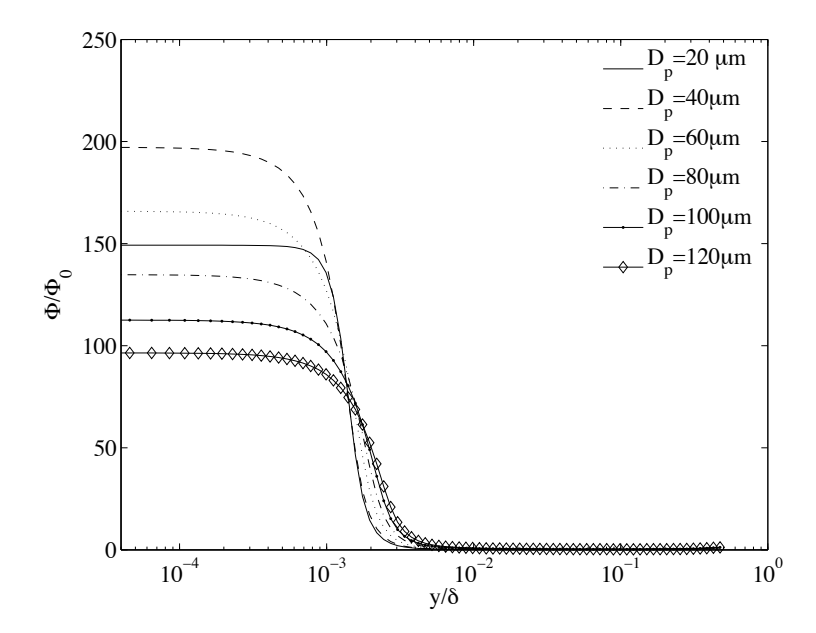


FIGURE 5.2. Mean particle volume fraction normalised with the initial particle volume fraction for six different particle diameters $\Phi_0 = 2 \cdot 10^{-4}$. Note the logarithmic scale in the wall normal direction.

5.1.3. The effect of particles on evolving pipe flow

An evolving upward gas-particle flow in a pipe is studied in paper 3. The aim is to investigate how the development length, i.e. the pipe length required for a flow to become fully developed, is affected by the presence of particles. In order answer this question a model simulation with the model presented in section 3.4 is performed and a simple estimation is derived from the particle momentum equation. The pipe length in the model simulations was 200 pipe diameters , D, long which was enough for the flow to become fully developed. Simulations were done for Stokes numbers between $\tau_p^+=34$ and 3950, mass loading from 0.5 to 1 and a Reynolds number of 24000. The development length is here defined as the distance to the inlet where the radial velocity profile differs less than 1% from the fully developed profile at 180 D.

To understand and to be able to predict the influence of the particle parameters on the development length a simple estimation was derived from the particle momentum equations and reads

$$\frac{l}{D} > \frac{DU}{T} \left(\frac{18\rho_g \nu_g}{\rho_p D_p^2} + \frac{24\Phi_p}{D_p} \sqrt{\frac{T}{\pi}} \right). \tag{5.1}$$

The development length, l, is expected to become shorter for increasing D_p and longer for increasing Φ_p according to this estimate. This estimation is

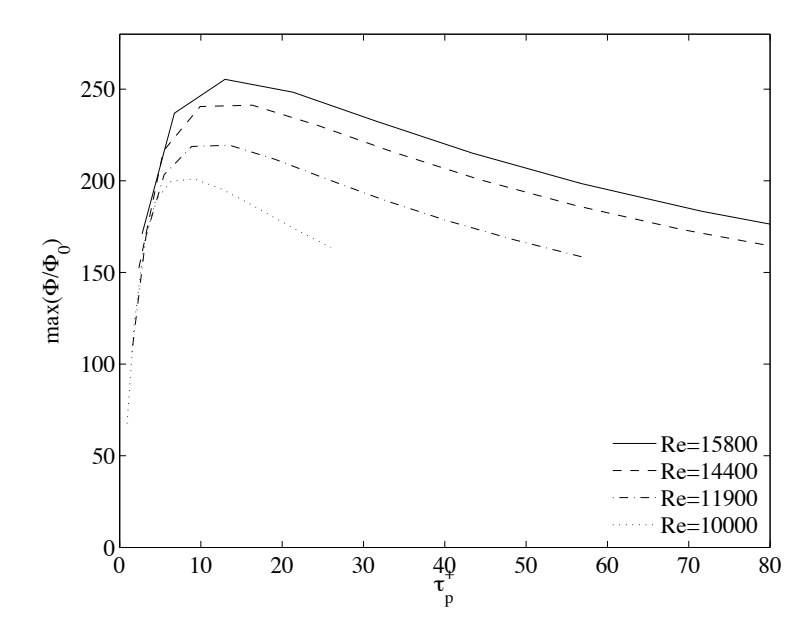


FIGURE 5.3. The maximum value of the mean particle volume fraction normalised with initial particle volume fraction in an upward vertical channel as a function of τ_p^+ for four different Reynolds numbers and $\Phi_0 = 1 \cdot 10^{-4}$.

shown as a function of D_p in figure 5.4a. In the same figure the development length obtained from model simulations is shown as a function of D_p for U_g , U_p and Φ_p . The inlet condition for the slip velocity $(U_p - U_g)$ is put equal to the final slip velocity at the outlet in order to neutralise the effect acceleration or deceleration of the particle velocity on the development length. The figure shows that the development length for small D_p is more than 3 times larger compared to an unladen case. As D_p increases the development length becomes shorter for all parameters because the coupling between the phases becomes weaker for larger particles. The results for the development length of U_p agree well with the estimation in equation 5.1.

In order to study the influence of the initial slip velocity model simulations were performed with a zero slip velocity at the inlet. In figure 5.4b these simulations are shown for the same cases as in figure 5.4a. For the gas phase velocity the results are the same as in figure 5.4a, whereas for Φ_p and U_p the development length decreases with particle diameter up to $D_p=100\mu m$ where it starts to increase substantially. For $D_p=300\mu m$ the development length is more than five times that of an unladen flow. This radical increase of the development length for large particles is due to the increasing final slip velocity with particle diameter. Since the larger particles initially are far from their

final slip velocity the distance required for the flow to become fully developed increases.

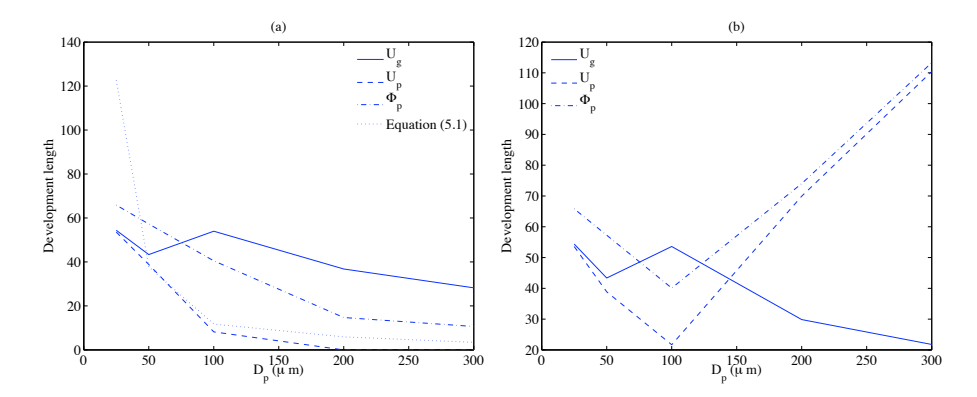


FIGURE 5.4. Development length, x/D, of the flow in an upward vertical pipe as a function of D_p for U_g , U_p and Φ_p . Effect of slip velocity taken into account (a). Zero initial slip velocity (b).

5.1.4. Modelling of K_p

Depending on particle volume fraction and Stokes number different models can be used to describe the particle turbulent kinetic energy, K_p . Hinze (1959) derived a simple model for K_p assuming that the particle velocity fluctuations only depends on the gas phase turbulence and the particle properties, i.e.

$$K_p = \frac{K_g}{1 + \frac{\tau_p}{T_r}}. (5.2)$$

Here $K_p < K_g$. However, it is known that for large particles the particle fluctuations can be larger than the gas phase turbulent fluctuations. Therefore, this simple model is only valid for small Stokes numbers, i.e. particles with small response times, and for rather dilute flows where the effect of particle-particle collisions are negligible. For larger Stokes numbers and particle volume fractions it is common to solve a transport equation for K_p using kinetic theory of granular flows in order to model the unclosed correlations by incorporating the micro-scale particle rheology as explained in paper 1 and 4. This approach gives good predictions of K_p in turbulent gas-particle flows for both larger St and Φ_p . For small St and Φ_p the prediction of K_p approaches equation (5.2) derived by Hinze (1959). In order to increase the parameter range where equation (5.2) is valid without having to solve a transport equation for K_p the model derived by Hinze (1959) was extended to include particle feedback and particle-particle collisions in paper 5. The collisions were represented by a Wiener process in the Langevin equation for the particle velocity. Solving the

equations with this modification gives a modified model for K_p

$$K_{p} = \frac{K_{g}}{1 + \frac{\tau_{p}}{T_{r}}} + \frac{3}{4}\nu_{tp}\tau_{p}(\frac{dU_{p}}{dy})^{2}$$
(5.3)

The last term on the R.H.S. of (5.3) is due to the introduction of particle-particle collisions in the Langevin equation of the particle phase.

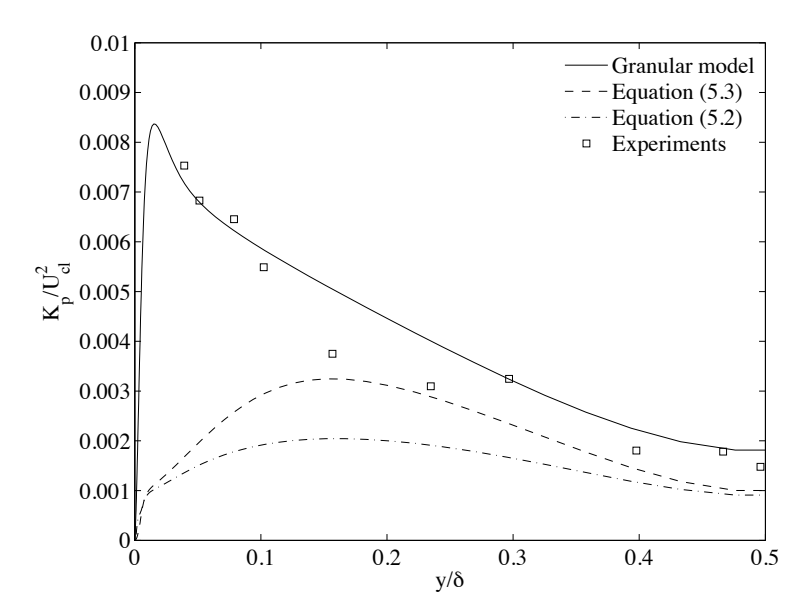


FIGURE 5.5. Turbulent kinetic energy normalised with the center line velocity in the presence of 50 μm glass particles with mass loading 10% shown for the two-fluid model using equation (5.2), (5.3) or kinetic theory of granular flows and experiments. $y^+ = \frac{yu_{\tau}}{\nu_g}$ is the distance to the wall in wall units where u_{τ} is the friction velocity.

Equation (5.2), (5.3) and the kinetic theory of granular flows have been implemented in the two-fluid model described in section 3.4. Figure 5.5 shows profiles of the particle turbulent kinetic energy normalised with the center line velocity as predicted by the three models and from experiments by Kulick et al. (1994). Using equation (5.3) instead of (5.2) increases K_p up to 50%. Compared to experiments the model using equation (5.3) agrees fairly well with experiments for $y^+ < 200$. However, the peak of K_p close to the wall is only captured by the model using kinetic theory of granular flows.

5.1.5. Backward-facing step

A more complex geometry approaching industrial applications is studied in paper 4. The purpose is to compare two different Eulerian-Eulerian gas-particle

models by simulating a turbulent particle-laden flow over a backward-facing step. In the first model the particle stress is obtained using the kinetic theory of granular flows and solves a transport equation for the particle fluctuating kinetic energy, K_p . In the second model a more simple approach is used. Here the particle stresses are obtained using a simple model both for the particle viscosity (Melville & Bray 1979) and K_p (Hinze 1959). It is assumed that the turbulence intensity of the particle phase is governed by the gas phase turbulence.

Profiles of both mean particle velocities and mean gas phase turbulent kinetic energy are compared with experimental data for different downstream positions in the backward-facing step. The main difference between the two models is that the first model slightly overpredicts the velocity and the second model underpredicts the gas turbulence intensity just after the expansion. However, the overall agreement between the two models and experimental data is good.

Outlook

The work presented in this thesis concerns prediction of turbulent gas-particle shear flows. A turbulent two-phase flow model based on the kinetic theory of granular flows that takes into account both particle feedback and particle-particle collisions has been derived. The model captures many fundamental flow phenomena very well and is used to investigate how particles affect turbulent wall-bounded flows.

The long term goal is to use turbulent gas-particle models to study engineering problems particularly within the energy sector where understanding of particle laden flows is of great importance. Examples of such flows are gasification and combustion of solid fuels in fluidized beds, catalytic cracking used to refine crude oil into petrol and gas-cleaning after combustion processes to prevent emissions of small particles. In many of these flows geometries are often complex, leading to very anisotropic flows. This will have a significant effect on the turbulence and on the particle fluxes, but these effects have not been taken into account in the present model. Highly anisotropic turbulent flows with strong mean shear and passive scalar fluxes can be accurately described by Explicit Algebraic Reynolds Stress Models (EARSM) and Explicit Algebraic Scalar Flux Models (EASFM). An idea is to apply this modelling approach to turbulent gas-particle flows. The stochastic model for particles in turbulent flows derived in paper 5 can be extended to anisotropic flows if the direction is taken into account in the derivation of the model.

Dense gas-particle flows are very complex due to the particle feedback and particle-particle collisions, examples of such flows are fluidized beds. In order to predict and develop dense flows in larger and more complex geometries Euler-Euler models are important tools since they are more efficient compared to Lagrangian particle models that only can predict dilute flows ($< 10^{-3}$) for larger geometries. The developed two-fluid model can be used to study more dense flows. However, in order to approach engineering problems issues like polydispersed solid particle diameters, particle rotation and particle-particle friction must be considered.



Acknowledgements

My supervisors Professor Gustav Amberg and Professor Arne Johansson are greatly acknowledged for their guidance. Their enthusiasm, patience and deep knowledge in physics have been invaluable. It has been a privilege being your student. Many thanks to Dr. Geert Brethouwer who has been involved during the project and given valuable feedback on my work that has improved it significantly. Thanks also to Dr. Minh Do-Quang for your patience answering numerous questions about femLego.

The project has been carried out in cooperation with Professor Alf-Erik Almstedt, Dr. Berend van Wachem and Aldo Benavides at Chalmers University. Regular feedback and fruitful discussions are gratefully acknowledged. The Swedish Energy Agency (Energimyndigheten) is acknowledged for financial support of the project.

Many thanks also to Andreas Carlson and Anders Dahlkild for providing valuable feedback on the manuscript. My room mates during the years Daniel Ahlman, Linus Marstorp, Florian von Stillfried and Peter Lenaers have contributed to a nice atmosphere, interesting discussions and a lot of laughter's. All friends and former and present colleges at the department have created a pleasant and helpful environment and brightened up my time here. Thank you! I also wish to thank my family and friends outside the department for your support and encouragement. You are all very important to me.

Last but not least I would like to express my deepest thanks to Ida and Nadja for your endless love, patience and support.



Division of work between authors

The research project was initiated by Gustav Amberg (GA) and Arne Johansson (AJ) who also acted as supervisors. GA, AJ, Geert Brethouwer (GB) and Tobias Strömgren (TS) have continuously discussed the progress of the project during the course of the work.

In paper 1, 2 and 3 the code development and calculations was done by TS with feedback from GA. The papers were written by TS with feedback from GB, GA and AJ.

Paper 4 was a collaboration with Aldo Benavides (AB) and Berend van Wachem (BW) at Chalmers university of technology. The code development and calculations was done by TS and AB. The paper was written by TS and AB with feedback from GB, BW, GA and AJ.

In paper 5 the derivation, code development and calculations where made by TS with input from GA. The paper was written by TS with feedback from GB, GA and AJ.



APPENDIX A

A.1. Code report

The turbulent gas-particle model based on the kinetic theory of granular flows, described in section 3.4, was implemented into fem Lego in cylindrical coordinates. A low Reynolds number $K-\omega$ model is used for the gas phase turbulence. The fem Lego Maple script for this model is shown on the the next pages. Turbulent gas-particle model based on the kinetic theory of granular flows in cylindrical coordinates

by Tobias Strömgren

For details see

A modelling study of evolving particle-ladden turbulent pipe-flow
T. Strömgren, G. Brethouwer, G. Amberg and A.V. Johansson
Submitted to Flow, Turbulence and Combustion, 2009.

```
L j:='j':
 Low- and high Reynolds number turbulence models.
   > ReTeq := CopyEq(ReT(r,z)=K(r,z)*Reno/omega(r,z));
                                                                                                           \textit{ReTeq} := \textit{CopyEq}\left(\textit{ReT}\left(r,z\right) = \frac{\textit{K}\left(r,z\right)\textit{Reno}}{\omega\left(r,z\right)}\right)
                                                                                                                                                                                                                                                                                                                                                                                                                                                                          (1.2)
 High Reynolds number model:
W REYDOUS HUMBER MOULE
alpha:= NoExpand(5/9*(1/10+ReT(r,z)/Rw)/(1+ReT(r,z)/Rw)*(1+ReT(r,z)/Rk)/(beta/3+ReT(r,z)/Rk));
(beta/3+ReT(r,z)/Rk));
alphas:= NoExpand(9/100*(5/18+(ReT(r,z)/Rk)/(1+ReT(r,z)/Rk));
Cmu := NoExpand(9/100*(5/18+(ReT(r,z)/Rbeta)^4)/(1+(ReT(r,z)/Rbeta)^4));
EPS:= Cmu*(r,z)*omega(r,z);
nut := alphas*K(r,z)/omega(r,z);
                                                             \alpha := NoExpand \left( \frac{5}{9} \frac{\left(\frac{1}{10} + \frac{ReT(r, z)}{Rw}\right) \left(1 + \frac{ReT(r, z)}{Rk}\right)}{\left(1 + \frac{ReT(r, z)}{Rw}\right) \left(\frac{1}{3} \beta + \frac{ReT(r, z)}{Rk}\right)} \right)
                                                                                                          Cmu := NoExpand
                                                                                                                                                                                      \frac{\frac{5}{18} + \frac{ReT(r,z)^4}{Rbeta^4}}{1 + \frac{ReT(r,z)^4}{1 + \frac{ReT
                                                                  EPS := NoExpand
                                                                                                                                                                                                                                                                                                               K(r,z)\omega(r,z)
                                                                                                                                                                                                      \frac{1}{3}\beta + \frac{ReT(r,z)}{Rk}
                                                                                                                                                                                                          1 + \frac{ReT(r,z)}{r}
                                                                                                                                                                                                                                                                                                                                                                                                                                                                          (1.3)
                                                                                                                                                                                                                               \omega(r,z)
 Turbulence model for the particle-phase
         > Kpgeq := CopyEq(Kpg(r,z) = (2*K(r,z)*3*T(r,z))^0.5);
                                                          \textit{Kpgeq} \coloneqq \textit{CopyEq} \left( \textit{Kpg} \left( r, z \right) = 2.449489743 \, \left( \textit{K} \left( r, z \right) \, \textit{T} \left( r, z \right) \right)^{0.5} \right)
                                                                                                                                                                                                                                                                                                                                                                                                                                                                          (1.4)
 Drag coefficient
```

```
 \begin{array}{lll} Rereq := CopyEq(Rer(r,z) = (2*pradius/dw*((U[1](r,z)-Up[1](r,z))^2+(U[2](r,z)-Up[2](r,z))^2+Rerin(r,z)^0.5)*Reno); \\ Schiller := 1+0.15*Rer(r,z)^0.(0.687); \\ Rerineq := CopyEq(Rerin(r,z) = t_Rerpos(2/3*(K(r,z)-Kpg(r,z)) + T(r,z))); \\ \end{array} 
     \textit{Rereg} \coloneqq \textit{CopyEq} \bigg( \textit{Rer} \left( r,z \right) = \frac{1}{\textit{dw}} \Big( 2 \, \textit{pradius} \, \Big( \left( U_1(r,z) - Up_1(r,z) \, \right)^2 + \left( U_2(r,z) \right)^2 + \left( U_2(r,z) \, \right)^2 + \left( 
                      -Up_2(r,z)\big)^2 + Rerin(r,z)\big)^{0.5} Reno\Big)\Big)
      Schiller := 1 + 0.15 \ Rer(r,z)^{0.687} Rerineq := CopyEq \left( Rerin(r,z) = \underline{t}_{-}Rerpos \left( \frac{2}{3} \ K(r,z) - \frac{2}{3} \ Kpg(r,z) + T(r,z) \right) \right)  (1.5)
Kinetic theory of granular flows

| Maximum packing of spheres
| Phimax := 0.64;
                                                                                                                                                                                                                                                                                                                                                                                                        (1.6)
   (1.7)
Non-dimensionalized particle diameter
  > Dp := 2*pradius/dw;
                                                                                                                                                           Dp := \frac{2 \ pradius}{dw}
                                                                                                                                                                                                                                                                                                                                                                                                        (1.8)
Time-scale of the gas-phase

> taug := 3/(2*omega(r,z));
                                                                                                                                                        taug := \frac{3}{2 \, \omega(r, z)}
                                                                                                                                                                                                                                                                                                                                                                                                        (1.9)
Collisional time-scale of the particle phase
     (1.10)
     taupceq := CopyEq \mid taupc(r, z)
                                  0.1476670429 \ pradius \left(1 - 1.160397208 \ \phi(r,z)^{1/3}\right) \sqrt{\frac{1}{T(r,z) + 0.000001}}
  Cheta := 1.8-1.35*(Ur[i](r,z) &t Up[i](r,z)/((Ur[1](r,z)^2+Ur[2](r,z) ^2+0.000001)^(0.5)*(Up[i](r,z)^2+Up[2](r,z)^2+0.000001)^(0.5)))^2;
                                                                                                                                                                                                                                                                                                                                                                                                 (1.11)
                      -\left(1.35\left(\mathit{Ur}_{1}(r,z)\;\mathit{Up}_{1}(r,z)+\mathit{Ur}_{2}(r,z)\;\mathit{Up}_{2}(r,z)\right)^{2}\right)\bigg/\Big(\left(\mathit{Ur}_{1}(r,z)^{2}+\mathit{Ur}_{2}(r,z)\right)^{2}\Big)
             + \ \mathcal{U}r_2(r,z)^2 + 0.000001\Big)^{1.0} \left(\ \mathcal{U}p_1(r,z)^2 + \mathcal{U}p_2(r,z)^2 + 0.000001\Big)^{1.0}\right) \\ \text{r.i.} := \ 3*(((Ur[1](r,z)^2+Ur[2](r,z)^2)^0.5)^2)/(2*K(r,z)+0.000001);
```

$$\xi := \frac{3\left(Ur_1(r,z)^2 + Ur_2(r,z)^2\right)^{1.0}}{2K(r,z) + 0.000001}$$
(1.12)

 $\overline{\underline{E}}$ ddy-particle interaction time-scale

> taupgteq := CopyEq(taupgt(r,z) = taug*(1+Cbeta*xi)^(-1/2));

taupgteq :=
$$CopyEq$$
 $\left(taupgt(r, z) = 3 \right) / \left(2 \omega(r, y)\right)$ (1.13)

$$\left(1 + \frac{1}{2 K(r,z) + 0.000001} \left(3 \right) \left(1.8\right)^{-1}\right)$$

$$-\left.\left(1.35\left(\mathit{Ur}_{1}(r,z)\;\mathit{Up}_{1}(r,z)+\mathit{Ur}_{2}(r,z)\;\mathit{Up}_{2}(r,z)\right)^{2}\right)\right/\left(\left(\mathit{Ur}_{1}(r,z)^{2}\right.\right.$$

$$\left. + \left. U r_2(r,z)^2 + 0.000001 \right)^{1.0} \left(\left. U p_1(r,z)^2 + U p_2(r,z)^2 + 0.000001 \right)^{1.0} \right) \right) \\ \left(\left. \left(U r_1(r,z)^2 + U r_2(r,z)^2 \right)^{1.0} \right) \right) \right)$$

#Inverse of the characteristic time scale of gas-particle momentum transfer taupgfInveq := CopyEq(taupgfInv(r,z) = (1+0.15*Rer(r,z)^0.687)/(St));

taupgfInveq := CopyEq (taupgfInv(r,z) =
$$\frac{1+0.15}{St}$$
 (1.14)

Particle-phase kinematic veiscosity

Nutpkeq := CopyEq(Nutpk(r,z)=(2/3*taupgt(r,z)*taupgfInv(r,z)*Kpg(r,z)+T(r,z)*(1+phi(r,z)*g0*2/5*(1+ep)*(3*ep-1)))*((2*taupgfInv(r,z)+2/5*(1+ep)*(3-ep)*taupc(r,z)))*(-1))*(-1);

$$Nupkeq := CopyEq \left(Nupk (r, z) \right)$$
 (1.15)

$$= \frac{1}{2 \ taupgflnv}(r,z) + \frac{2}{5} \frac{(1+ep) \ (3-ep)}{taupc(r,z)} \left(\frac{2}{3} \ taupgf(r,z) \ taupgflnv}(r,z) + \frac{2}{5} \frac{(1+ep) \ (3-ep)}{taupc(r,z)} \left(\frac{2}{3} \ taupgf(r,z) \ taupgflnv}(r,z) + \frac{2}{5} \frac{\phi(r,z) \ (1+ep) \ (3-ep-1)}{1-1.160397208 \ \phi(r,z)^{1/3}} \right) \right)$$
Particle-phase viscosity due to collisions
$$> \text{Nupceq} := \text{CopyEq}(\text{Nupc}(r,z) = \frac{4}{5} \frac{1}{1-1.160397208 \ \phi(r,z)^{1/3}} \left(\phi(r,z) \ (1 - ep)^{2}(\text{T}(r,z) + 0.000001)/3.14)^{2}(-5); \right)$$

$$Nupceq := \text{CopyEq} \left(\text{Nupc}(r,z) = \frac{4}{5} \frac{1}{1-1.160397208 \ \phi(r,z)^{1/3}} \left(\phi(r,z) \ (1 - ep)^{2}(-1.60397208 \ \phi(r,z))^{1/3} \right) \right)$$

$$+ \frac{2 \ pradus}{1-1} \left(0.3184713376 \ T(r,z) + 3.184713376 \ 10^{-8} \right)^{0.5} \right) \right)$$

$$\text{Diffusion coefficient}$$

$$> \text{kappateq} := \text{CopyEq}(\text{kappat}(r,z) = \frac{(3/5*\text{Kpg}(r,z)*\text{taupgf}(r,z)*\text{taupgfInv}(r,z) + (1/2)^{-8} \right) }{dw}$$

$$> \frac{1}{1-1.160397208} \left(\frac{1}{5} \frac$$

$$\begin{bmatrix} ElementInt\left(\eta(r,z)\ Ur_1(r,z)\right) = ElementInt\left(\eta(r,z)\ \left(U_1(r,z) - Up_1(r,z)\right)\right) \\ + ElementInt\left(\frac{1}{3}\ \eta(r,z)\ Kpg\left(r,z\right)\ taupgt\left(r,z\right) \\ \hline \left(\frac{\partial}{\partial r}\ \phi(r,z) + \frac{\partial}{\partial r}\ \phi(r,z)\right) \\ ElementInt\left(\eta(r,z)\ Ur_2(r,z)\right) = ElementInt\left(\eta(r,z)\ \left(U_2(r,z) - Up_2(r,z)\right)\right) \\ + ElementInt\left(\frac{1}{3}\ \eta(r,z)\ Kpg\left(r,z\right)\ taupgt\left(r,z\right) \\ \hline \left(\frac{\partial}{\partial z}\ \phi(r,z) + \frac{\partial}{\partial z}\ \phi(r,z)\right) \\ \hline Other stuff \\ \begin{bmatrix} > \ e[1] \ := \ 0; \\ e[2] \ := \ 1; \\ \hline e_1 := \ 0 \\ e_2 := 1 \\ \end{bmatrix}$$

$$(1.20)$$

▼ Specify PDEs

▼ Distance function

Describes the distance to solid walls using a function

| disteq:=CopyEq(distr(r,z)=t_distr(r,Rad));
| disteq:=CopyEq(distr(r,z) = t_distr(r,Rad)) | (2.1.1)

▼ Gas-velocity equation

$$Veg_1 = ElementInt \left(\frac{r^2 \left(1 - \phi \theta(r, z) \right) \eta(r, z) \left(U_1(r, z) - U \theta_1(r, z) \right)}{dt} \right) \\ + ElementInt \left(r^2 \eta(r, z) \left(1 - \phi \theta(r, z) \right) \left(U \theta_1(r, z) \left(\frac{\partial}{\partial r} U_1(r, z) \right) + U \theta_2(r, z) \right) \right) \\ = -ElementInt \left(\frac{\partial}{\partial r} U_1(r, z) \right) \right) = \\ -ElementInt \left(\frac{1}{rhog} \left(r^2 \left(1 - \phi \theta(r, z) \right) \eta(r, z) \left(2 \left(\frac{\partial}{\partial r} \rho \theta(r, z) \right) \right) \right) \\ - \left(\frac{\partial}{\partial r} \rho \theta \theta(r, z) \right) \right) \right) - ElementInt \left(\frac{1}{Reno} \right) \\ - \left(\frac{\partial}{\partial r} \rho \theta \theta(r, z) \right) \right) \right) - ElementInt \left(\frac{1}{Reno} \right) \\ + \frac{NoExpand}{1 + \frac{ReT(r, z)}{Rk}} \left(\frac{1}{h} \frac{ReT(r, z)}{Rk} \right) \left(1 - \phi \theta(r, z) \right) \right) \\ + \left(\frac{\partial}{\partial r} U_1(r, z) \right) \left(\frac{\partial}{\partial z} \eta(r, z) \right) + \left(\frac{\partial}{\partial z} U_1(r, z) \right) \left(\frac{\partial}{\partial z} \eta(r, z) \right) \\ + \left(\frac{\partial}{\partial r} U_2(r, z) \right) \left(\frac{\partial}{\partial z} \eta(r, z) \right) \right) + 2 U_1(r, z) \eta(r, z) \right) \\ - ElementInt \left(\frac{2}{3} r^2 \eta(r, z) \left(- \left(\frac{\partial}{\partial r} \phi \theta(r, z) \right) K \theta(r, z) + \left(1 - \phi \theta(r, z) \right) \right) \\ + r \left(\frac{\partial}{\partial r} K \theta(r, z) \right) \right) NoExpand \left(\frac{1}{3} \beta + \frac{ReT(r, z)}{Rk} \right) \\ + r \left(\frac{\partial}{\partial r} U \theta_1(r, z) \right) + r^2 \left(\frac{\partial}{\partial z} U \theta_2(r, z) \right) \right) \\ - ElementInt \left(\frac{r^2 \eta(r, z) \left(1 + 0.15 Rer(r, z)^{0.687} \right) rhop \phi \theta(r, z) Ur_1(r, z)}{rry r} \right)$$

$$Ueq_{2} := ElementInt \left(\frac{r \left(1 - \phi\theta(r,z) \right) \eta(r,z) \left(U_{2}(r,z) - U\theta_{2}(r,z) \right)}{dt} \right)$$

$$+ ElementInt \left(r \eta(r,z) \left(1 - \phi\theta(r,z) \right) \left(U\theta_{1}(r,z) \left(\frac{\partial}{\partial r} U_{2}(r,z) \right) + U\theta_{2}(r,z) \right) \right)$$

$$= -ElementInt \left(\frac{1}{rhog} \left(r \left(1 - \phi\theta(r,z) \right) \eta(r,z) \left(2 \left(\frac{\partial}{\partial z} \rho\theta(r,z) \right) \right) \right) \right)$$

$$- \left(\frac{\partial}{\partial z} \rho\theta\theta(r,z) \right) \right) \right) - ElementInt \left(\frac{1}{Reno} \right)$$

$$+ \frac{NoExpand}{show (r,z)} \left(\frac{1}{3} \beta + \frac{ReT(r,z)}{Rk} \right) K(r,z) \right)$$

$$+ \frac{1}{show (r,z)} \left(\frac{\partial}{\partial r} \eta(r,z) \right) + 2 \left(\frac{\partial}{\partial z} U_{2}(r,z) \right) \left(\frac{\partial}{\partial z} \eta(r,z) \right) + \left(\frac{\partial}{\partial z} U_{1}(r,z) \right)$$

$$+ \left(1 - \phi\theta(r,z) \right) \left(\frac{\partial}{\partial z} K\theta(r,z) \right) \right) \right) + ElementInt \left(\frac{2}{3} r \eta(r,z) \left(- \left(\frac{\partial}{\partial z} \phi\theta(r,z) \right) K\theta(r,z) \right)$$

$$+ \left(1 - \phi\theta(r,z) \right) \left(\frac{\partial}{\partial z} K\theta(r,z) \right) \right) NoExpand \left(\frac{1}{3} \beta + \frac{ReT(r,z)}{Rk} \right) K(r,z) \left(U\theta_{1}(r,z) \right)$$

$$+ r \left(\frac{\partial}{\partial r} U\theta_{1}(r,z) \right) + r \left(\frac{\partial}{\partial z} U\theta_{2}(r,z) \right) \right) \right)$$

$$- ElementInt \left(\frac{r \eta(r,z) \left(1 + 0.15 Rer(r,z)^{0.687} \right) rhop \phi\theta(r,z) Ur_{2}(r,z)}{rhog Si} \right)$$

$$+ Particle-velocity equation$$

```
 \begin{aligned} & (\text{Up}[1](r,z))[k])) = \\ & = \text{ElementInt}(\text{rcn*phi0}(r,z)*\text{rhog/rhop*eta}(r,z)*\text{nab\_cc}(2*\text{p0}(r,z))[1]) \\ & = \text{ElementInt}((0*\text{Acrivos}(r,z)*\text{chifp*Nutpk}(r,z)*\text{Nupc}(r,z))*\text{phi0}(r,z))*\text{cr.} \\ & (r,z)*(\text{rcn.}) & (r,z)*\text{con.} \\ & (r,z)*(\text{li}) & (r,z)*\text{con
```

$$-ElementInt\left(\frac{1}{rhop}\left(r\phi\theta(r,z)\ rhog\ \eta(r,z)\right)\left(2\left(\frac{\partial}{\partial z}\ p\theta\theta(r,z)\right)\right)\right) - ElementInt\left((xdifp+Nutpk\ (r,z)+Nutpc\ (r,z))\right)\right) - ElementInt\left((xdifp+Nutpk\ (r,z)+Nutpc\ (r,z))\right)\right)$$

$$= (1) \phi\theta(r,z)\ r\left(\left(\frac{\partial}{\partial r}\ Up_2(r,z)\right)\left(\frac{\partial}{\partial r}\ \eta(r,z)\right)\right) + 2\left(\frac{\partial}{\partial z}\ Up_2(r,z)\right)\left(\frac{\partial}{\partial r}\ \eta(r,z)\right)\right)\right)$$

$$= ElementInt\left(\frac{2}{3}\ r\eta(r,z)\right)\left(\left(\frac{\partial}{\partial z}\ \phi\theta(r,z)\right)\ T(r,z)\right) + \phi\theta(r,z)\left(\frac{\partial}{\partial z}\ T(r,z)\right)\right) + ElementInt\left(\frac{2}{3}\ \phi\theta(r,z)\right)\left(\frac{\partial}{\partial z}\ \eta(r,z)\right)\left(xdifp+Nutpk\ (r,z)\right)$$

$$= \frac{3}{2}\ Nutpc\ (r,z)\right)\left(Up\theta_1(r,z)+r\left(\frac{\partial}{\partial r}\ Up\theta_1(r,z)\right)+r\left(\frac{\partial}{\partial z}\ Up\theta_2(r,z)\right)\right) + ElementInt\left(\frac{r\eta(r,z)\left(1+0.15\ Rer(r,z)\right)^{0.687}}{Sr}\right)\phi\theta(r,z)\ Ur_2(r,z)}{Sr}\right)$$

$$= ElementInt\left(r\eta(r,z)\phi\theta(r,z)\ Fr\right)$$

$$= BoundaryInt\left(\frac{1}{1-1.160397208\ \phi(r,z)^{1/3}}\left(0.8177083333\ gBCval\ r\eta(r,z)\right)\right)$$

$$= \frac{1}{1-1.160397208\ \phi(r,z)^{1/3}}\left(0.81770833333\ gBCval\ r\eta(r,z)\right)$$

$$= \frac{1}{1-1.160397208\ \phi(r,z)}\left(\frac{1}{1-1.160397208\ \phi(r,z)\right)$$

$$= \frac{1}{1-1.160397208\ \phi(r,z)}\left(\frac{1}{1-1.160397208\ \phi(r,z)}\right)$$

$$= \frac{1}{1-1.160397208\ \phi(r,z)}\left(\frac{1}{1-1.160397208\ \phi(r,z)}\right)$$

$$= \frac{1}{1-1.160397208\ \phi(r,z)}\left(\frac{1}{1-1.160397208\ \phi(r,z)}\right)$$

$$= \frac{1}{1-1.160397208\ \phi(r,z)}\left(\frac{1}{1$$

```
-dt*ElementInt(r*nab_cc(p(r,z)-p0(r,z))[k]*eta(r,z));
         \begin{aligned} & \text{Uceq}_1 := \text{ElementInt} \left( r \ Uc_1(r,z) \ \eta(r,z) \right) = \text{ElementInt} \left( r \ U_1(r,z) \ \eta(r,z) \right) \\ & - \text{dt ElementInt} \left( r \left( \frac{\partial}{\partial r} \ p(r,z) - \left( \frac{\partial}{\partial r} \ p\theta\left(r,z\right) \right) \right) \eta(r,z) \right) \end{aligned}
       \textit{Uceq}_2 \coloneqq \textit{ElementInt}\left(r \; \textit{Uc}_2(r,z) \; \eta(r,z)\right) = \textit{ElementInt}\left(r \; \textit{U}_2(r,z) \; \eta(r,z)\right)
                                                                                                                                                                                                                                                                                                                                                                                                                                                                                                                   (2.5.1)
                                  - dt \, \textit{ElementInt} \left( r \left( \frac{\partial}{\partial z} \, p(r,z) - \left( \frac{\partial}{\partial z} \, p \theta(r,z) \, \right) \right) \eta(r,z) \, \right)
Pressure eqns
 > # solve for p(r,z);

> # NOTE: add BoundaryInt for open boundaries with pressure prescribed
                            pPoisseq := ElementInt \left( r \left( \frac{1 - \phi \theta(r, z)}{rhog} + \frac{\phi \theta(r, z)}{rhop} \right) \left( \left( \frac{\partial}{\partial r} p(r, z) \right) \right) - \left( \frac{\partial}{\partial r} p(r, z) \right) - \left( \frac{\partial}{\partial r} p(r, z) \right) \left( \frac{\partial}{\partial r} \eta(r, z) \right) + \left( \frac{\partial}{\partial z} p(r, z) \right) - \left( \frac{\partial}{\partial r} p(r, z) \right) - \left( \frac{\partial}{\partial r}
                                                                                                                                                                                                                                                                                                                                                                                                                                                                                                                  (2.6.1)
                           z)\bigg)\left(\frac{\partial}{\partial z}\,\eta(r,z)\right)-\left(\frac{\partial}{\partial z}\,p\theta(r,z)\right)\left(\frac{\partial}{\partial z}\,\eta(r,z)\right)\bigg)\bigg)=\frac{1}{dt}\bigg(
                           -ElementInt\left(r\,\eta(r,z)\left(-\left(\frac{\partial}{\partial r}\,\phi\theta(r,z)\right)\right)U_1(r,z)+\left(1-\phi\theta(r,z)\right)U_2(r,z)\right)
                        z)\big)\left(\frac{\partial}{\partial r}\;U_{1}(r,z)\right)+\left(\frac{\partial}{\partial r}\;\phi\theta(r,z)\right)U_{P_{1}}(r,z)+\phi\theta(r,z)\left(\frac{\partial}{\partial r}\;U_{P_{1}}(r,z)\right)
                         -\left(\frac{\partial}{\partial z}\phi\theta(r,z)\right)U_{2}(r,z)+\left(1-\phi\theta(r,z)\right)\left(\frac{\partial}{\partial z}U_{2}(r,z)\right)+\left(\frac{\partial}{\partial z}\phi\theta(r,z)\right)U_{2}(r,z)+\phi\theta(r,z)\left(\frac{\partial}{\partial z}U_{2}(r,z)\right)+\left(1-\phi\theta(r,z)\right)U_{1}(r,z)\eta(r,z)
                            \begin{split} &+\phi\theta(r,z)\;\textit{Up}_{1}(r,z)\;\eta(r,z)\left)-\textit{ElementInt}\left(1\right)\;\textit{eps\_p ElementInt}\left(r\left(\left(\frac{\partial}{\partial r}\;p\left(r,z\right)\right)\left(\frac{\partial}{\partial z}\;\eta(r,z)\right)+\left(\frac{\partial}{\partial z}\;p\left(r,z\right)\right)\left(\frac{\partial}{\partial z}\;\eta(r,z)\right)\right)\right)\right) \end{split}
```

$$Keq := ElementInt \left(\frac{r\eta(r,z) \left(1 - \phi(r,z) \right) \left(K(r,z) - K\theta(r,z) \right)}{dt} \right)$$

$$+ ElementInt \left(r\eta(r,z) \left(1 - \phi(r,z) \right) \left(Uc_1(r,z) \left(\frac{\partial}{\partial r} K(r,z) \right) + Uc_2(r,z) \right) \right)$$

$$= \left(\frac{\partial}{\partial z} K(r,z) \right) \right) = ElementInt \left(\frac{1}{\omega(r,z)} \left(2 r\eta(r,z) \left(1 - \phi(r,z) \right) \right) \right)$$

$$= \left(\frac{1}{3} \beta + \frac{ReT(r,z)}{Rk} \right)$$

$$= \left(\frac{1}{3} \beta + \frac{ReT(r,z)}{Rk} \right)$$

$$= \left(\frac{\partial}{\partial r} Uc_1(r,z) \right)^2$$

$$+ \left(\frac{\partial}{\partial r} Uc_2(r,z) \right)^2 + \left(\frac{\partial}{\partial r} Uc_2(r,z) \right) \left(\frac{\partial}{\partial z} Uc_1(r,z) \right)$$

$$+ \left(\frac{\partial}{\partial r} Uc_2(r,z) \right)^2 + \left(\frac{\partial}{\partial z} Uc_2(r,z) \right)^2 \right) \right)$$

$$= \left(\frac{\partial}{\partial r} Uc_2(r,z) \right)^2 + \left(\frac{\partial}{\partial z} Uc_2(r,z) \right)^2 \right)$$

$$= \left(\frac{\partial}{\partial r} Uc_2(r,z) \right)^2 + \left(\frac{\partial}{\partial z} Uc_2(r,z) \right)^2 \right)$$

$$= \left(\frac{\partial}{\partial r} Uc_1(r,z) \right)$$

$$= \left(\frac{\partial}{\partial r} Uc_2(r,z) \right)^2 + \left(\frac{\partial}{\partial z} Uc_2(r,z) \right)^2 \right)$$

$$= \left(\frac{\partial}{\partial r} Uc_1(r,z) \right)$$

$$= \left(\frac{\partial}{\partial r} Uc_2(r,z) \right)$$

$$=$$

▼ T-equation

z)
$$\phi(r,z) \left(1 - ew^2\right) \sqrt{3} \ T\theta(r,z)^{3/2}$$
)
+ ElementInt $\left(\frac{1}{Sr} \left(r \eta(r,z) \left(1 + 0.15 \ Rer(r,z)^{0.687}\right) \phi(r,z) \ (Kpg(r,z) - 3 \ T(r,z))\right)\right)$

▼ Omega-equation

$$NoExpand \left(\frac{5}{9} \frac{\left(\frac{1}{10} + \frac{ReT(r,z)}{Rw} \right) \left(1 + \frac{ReT(r,z)}{Rk} \right)}{\left(1 + \frac{ReT(r,z)}{Rw} \right) \left(\frac{1}{3} \beta + \frac{ReT(r,z)}{Rk} \right)} \right)$$

$$NoExpand \left(\frac{1}{2} \left(\frac{1}{2} + \frac{ReT(r,z)}{Rk(3)} \beta \right) + \frac{ReT(r,z)}{Rk} \right) \right) \left(\frac{\partial}{\partial r} Uc_1(r,z) \right)^2$$

$$+ \frac{1}{2} \left(\frac{\partial}{\partial z} Uc_1(r,z) \right)^2 + \left(\frac{\partial}{\partial r} Uc_2(r,z) \right) \left(\frac{\partial}{\partial z} Uc_1(r,z) \right)$$

$$+ \frac{1}{2} \left(\frac{\partial}{\partial r} \eta(r,z) \right) \left(\frac{\partial}{\partial r} omeT(r,z) \right) \right) - ElementInt \left(1 - \phi(r,z) \right)$$

$$Reno$$

$$+ \frac{\left(\frac{\partial}{\partial z} \eta(r,z) \right) \left(\frac{\partial}{\partial z} omeT(r,z) \right)}{Reno} \right) - ElementInt \left(\frac{1}{\omega(r,z)} \left(r \right) \right)$$

$$- \phi(r,z) \right) NoExpand \left(\frac{1}{3} \beta + \frac{ReT(r,z)}{Rk} \right) K(r,z) \sigma \left(\left(\frac{\partial}{\partial r} \eta(r,z) \right) \right)$$

$$- ElementInt \left(\frac{1}{\omega(r,z)} \left(r \right) - \phi(r,z) \right) NoExpand \left(\frac{1}{3} \beta + \frac{ReT(r,z)}{Rk} \right) K(r,z) \sigma \left(\left(\frac{\partial}{\partial r} \eta(r,z) \right) \right)$$

$$- ElementInt \left(\frac{1}{\omega(r,z)} \left(r \right) - \phi(r,z) \right) \left(\frac{\partial}{\partial r} omeT(r,z) \right) \right)$$

$$- ElementInt \left(\frac{1}{\alpha(r,z)} \frac{ReT(r,z)}{Rk} \right) K(r,z) \sigma \left(\left(\frac{\partial}{\partial r} \eta(r,z) \right) \left(\frac{\partial}{\partial r} omegaw(r,z) \right) + \left(\frac{\partial}{\partial r} \eta(r,z) \right) \left(\frac{\partial}{\partial r} omegaw(r,z) \right) \right)$$

$$- ElementInt \left(\frac{1}{rhog St} \left(\frac{1}{rhog St} \left(\frac{1}{rhog St} \right) \left(\frac{1}{rhog St} \left(\frac{1}{rhog St} \right) \left(\frac{1}{rhog St} \right)$$

```
| +0.15 Rer(r, z) 0.687 | rhop φ(r, z) ω(r, z) (2 K(r, z) - Kpg(r, z))) |
| walleq = CopyEq(omegaw(r, z) = i_OmeWall(Reno, distr(r, z), omega_wall, β)) (2.9.1)
| Define input list |
| **set up lists | eq_list:= subs((omega(r, z) = omeT(r, z) + omegaw(r, z), [Ueq[1], Ueq[2], Upq[1], Upq[2], ppoisseq, poldeq, phieq, disteq, Ucq[1], Ucq[2], keq, omegaeq, walleq, ReTeq, Rereq, Kpgq, Teq, Nutpkeq, Nupcq, kappateq, Verq[1], Urq[2], taupceq, taupgeq, taupgfinveq, Rerineq]; | Urq[2], taupceq, taupgeq, taupgfinveq, Rerineq]; | Urq[2], taupceq, taupgfinveq, Rerineq]; | unknown list:= [U[1](r,z), U[2](r,z), Up[1](r,z), Up[2](r,z), pqum(r,z), ReT(r,z), Rer(r,z), Kpg(r,z), T(r,z), Nutpk(r,z), Nupc(r,z), kappat(r,z), mapaw(r,z), Rerin(r,z)]; | (U[1](r,z), Up[2](r,z), Upq[2](r,z), Omega(r,z), Rerin(r,z); | (U[1](r,z), Upq[2](r,z), Upq[2](r,z), PQ(r,z), PQ(r,z)
```

```
Uin := Uo
                                                                                                                                                                                                                                                                                                               Upin := Upo
                                                                                                                                                                                                                                                                                                                                                                                                                                                                                                                                                                                                                                                                                                                (4.1)
                                                                                                                                                                                                                                                                                    Omegain := omegao
                                                                                                                                                                 > dirbclist:=[ c
                 \textit{dirbclist} := \left| \textit{omegaw}(r, z) = \underline{t} \cdot \textit{OmeWall} \left( \textit{Reno, distr}(r, z), \textit{omega\_wall}, \beta \right), U_2(r, z) \right|
                                                                                                                                                                                                                                                                                                                                                                                                                                                                                                                                                                                                                                                                                                                (4.2)
                                                   =qBCval\ Uo,\ U_1(r,z)=0,\ Uc_2(r,z)=qBCval\ Uo,\ Uc_1(r,z)=0,\ Up_2(r,z)
                                                   =qBCval\ Upo,\ Up_{1}(r,z)=0,\\ \phi(r,z)=qBCval\ phi\_in,\ K\left(r,z\right)=Ko\ qBCval,\ T\left(r,z\right)
                                                 =\frac{2}{3} \text{ Ko qBCval, omeT}(r, z) = \text{omegao qBCval, } p(r, z) = -\frac{2}{3} \text{ qBCval } K(r, z)
                 => mkDirBC2(dirbclist,unknown_list,old_unknown_list, params_list, unkntestlist,testbsflist);
                   1, \ | \textit{DirBC} = 0, \textit{DirBC} = \textit{qBCval}_1 \ \textit{qqP}_9, \textit{DirBC} = 0, \textit{DirBC} = \textit{qBCval}_1 \ \textit{qqP}_{10}, \textit{DirBC} = 0, \text{DirBC} = \text{qBCval}_1 \ \textit{qqP}_{10}, \text{DirBC} = \text{qBCval}_1 \ \textit{qqP}_1 \
                                                 -\frac{2}{3} \left. qBCval_1 \right. u_{node, \, 11}, DirBC = \left. qBCval_1, DirBC = \left. qBCval_1 \right. qqP_{24}, DirBC = \left. qBCval_1, DirBC \right. 
                                               DirBC = 0, DirBC = qBCval_1 \ qqP_9, DirBC = qqP_{18} \ qBCval_1, DirBC = qqP_{19} \ qBCval_1, \\
                                               DirBC = t\_OmeWall\left(\left.qqP_1, u_{node,\,8}, qqP_{12}, qqP_{13}\right), DirBC = qBCval_1, DirBC
                                                 =qBCval_1, DirBC = qBCval_1, DirBC = \frac{2}{3} \ qqP_{18} \ qBCval_1, DirBC = qBCval_1, DirBC
                                                   =qBCval_1, DirBC = qBCval_1, DirBC = qBCval_1,
                                               DirBC = qBCval_1, DirBC = qBCval_1, DirBC = qBCval_1, DirBC = qBCval_1
                                                                                                                                                                                                                                                                                                                               adddbc
                                                                                                                                                                                                                                                                                                                                                                                                                                                                                                                                                                                                                                                                                                                  (4.3)
Specify input
```

```
> #get files to read input from Gmsh's meshfile;
    #getGmshInput(params list):
> #get files to read input from femLab's meshfile;
#getFemLabInput(params list):
    #getDneutralInput(params list):
    SimpleMeshInput(params_list):
```

▼ Initial Conditions

```
LL
                                                          ic_init
                                                                                                                           (6.2)
▼ Specify output
         plotlist:=[[U[1](r,z),U[2](r,z)], p(r,z), [Up[1](r,z),Up[2](r,z)], K(r,z), omeT(r,z), omegaw(r,z), phi(r,z), Rer(r,z), ReT(r,z), Kpg(r,z), T(r,z), Nupc(r,z), Nupc(r,z), Kappac(r,z), Up(1](r,z), Up(2](r,z), taupc(r,z), taupgt(r,z), taupgf(r,z), Rerin(r,z)],
    plotlist := \left[ \left[ U_{1}(r,z), U_{2}(r,z) \right], p(r,z), \left[ Up_{1}(r,z), Up_{2}(r,z) \right], K(r,z), omeT(r,z), \right]  (7.1)
         omegaw(r, z), \phi(r, z), Rer(r, z), ReT(r, z), Kpg(r, z), T(r, z), Nutpk(r, z),
         \textit{Nupc}\,(r,z), \textit{kappat}\,(r,z), \textit{kappac}\,(r,z), \left[\textit{Ur}_1(r,z), \textit{Ur}_2(r,z)\right], \textit{taupc}\,(r,z),
         taupgt(r, z), taupgfInv(r, z), Rerin(r, z)
        menulist:=[vel, p, velp, K, omega, omegaw, phi, Rer, ReT, Kpg, T, Nutpk,
Nupc, kappat, kappac, Urel, taupc, taupgt, taupgfInv, Rerin];
    menulist := [vel, p, velp, K, \omega, omegaw, \phi, Rer, ReT, Kpg, T, Nutpk, Nupc, kappat, kappac,
                                                                                                                           (7.2)
         Urel, taupc, taupgt, taupgfInv, Rerin
         OpenDXPlotP1(plotlist,menulist,unknown_list,old_unknown_list,params_list,
triangles);
                                                        wroutp();
                                                    outputresults();
                                                          true
                                                                                                                           (7.3)
   Specify linear algebra solvers
   > # set up different solvers to use with different equations:
        solve_list:=[gmres, gmres, gmres, gmres, iccg, copy, iccg, copy, iccg, iccg, gmres, gmres, copy, copy; mkSolve(solve_list,eq_list,unknown_list);
                                                         solve.c:
                                                          false
                                                                                                                           (8.1)
Create the core of the solver
    -> domatrixfree;
                                                          false
                                                                                                                           (9.1)
   mkresi
                                                         amedsn
                                                          adidsp
                                                          uzadsp
                                                          addr1
                                                         addm1
                                                          addr2
```

addm2

addr3

addm3

addr4

addm4

addr5

addm5

addr6

addr7 addm7

addr8

addr9

addm9

addr10

addm10addr11

addm11

addr12 addm12

addr13

addr14

addr15

addr16

addr17 addm17

addr18 addr19

addr20

addr21

addr22

addm22

addr23

addm23

addr24

addr25

addr26

addr27 adbr1

adbm1

adbr2

adbm2

adbr3

adbm3

adbr4 adbm4

adbr5

adbm5

adbr6

adbm6

adbr7

adbm7 adbr8

adbm8

adbr9

adbm9

adbr10

adbm10 adbr11

adbm11

adbr12

adbm12

adbr13

adbm13

adbr14

adbm14

adbr15

adbm15

adbr16

adbm16 adbr17

adbm17

adbr18

adbm18

adbr19

adbm19 adbr20

```
adbm20
                                        adbr21
                                       adbm21
                                        adbr22
                                       adbm22
                                        adbr23
                                       adbm23
                                        adbr24
                                       adbm24
                                        adbr25
                                       adbm25
                                        adbr26
                                       adbm26
                                        adbr27
                                       adbm27
                                        grbcrs
                                        bdedsp
                                        addini
                                     include/size.h
                                     include/csize.h
                                changing jacobians list:
true, true, true, true, true, true, true, true, false, false, true, true, true, true, true, true, true,
   true, true, true, true, false, false, true, true, true, true
                           size_parameters := [27, 27, 6, 3]
                                                                                         (9.2)
   size_parameters;
                                    [27, 27, 6, 3]
                                                                                          (9.3)
```

Instructions on how to compile and run

```
# Done!
# Save the worksheet. The Maple session is now complete.
# The following steps are done in the unix shell:
# Compile the source code by typing make.
# Copy indata_sample to indata (say), edit indata to contain the input you want.
# Run the program by typing ./femlego
# view the results using for example Matlab, ParaView, OpenDX, ...
```

Important! In order to keep K(r,z), ome T(r,z) and T(r,z) positive close to the wall initially write the following after each varible in source/solve.c:

```
Example for K(r,z), variable number 11:
```

for(ii=0;ii<totalunk;ii++){

```
if(u[ii+totalunk*10]<0){
u[ii+totalunk*10]=0;
}
```

Do this after the maple document has been compiled and re-compile the C++ code.

Bibliography

- ACHENBACH, E. 1974 Vortex shedding from spheres. J. Fluid Mech. 62, 209–221.
- Amberg, G., Törnhardt, R. & Winkler, C. 1999 Finite element simulations using symbolic computing. *Mathematics and Computers in Simulation* 17, 228–237.
- Anderson, T. & Jackson, R. 1967 A fluid mechanical description of fluidized beds. *Ind. Engng. Chem. Fundam.* **6**, 527–539.
- ARCEN, B., Tanière, A. & ZAICHIK, L. 2008 Assessment of a statistical model for the transport of discrete particles in a trubulent channel flow. *Int. J. Multiphase Flow* **34**, 419–426.
- Bagnold, R. A. 1954 Experiments on gravity-free dispersion of large solid spheres in a newtonian fluid under shear. *Proc. R. Soc. London Ser. A* 225, 49–63.
- Balzer, G., Simonin, O., Boelle, A. & Lavieville, J. 1996 A unifying modelling approach for the numerical prediction of dilute and dense gas-solid two-phase flow. *Tech. Rep.* Département Laboratoire National d'Hydraulique.
- Benavides, A. 2008 Eulerian-Eulerian modeling of turbulent gas-particle flow. *Tech. Rep.* Department of Applied Mechanics, Chalmers University of Technology, Göteborg Sweden.
- Benavides, A. & van Wachem, B. 2008 Numerical simulation and validation of dilute turbulent gas-particle flow with inelastic collisions and turbulence modulation. *Powder technology* **182**, 294–306.
- Benyahia, S., Syamlal, M. & O'Brien, T. J. 2007 Study of the ability of multiphase continuum models to predict core-annulus flow. *AIChE J.* **53**, 2549–2568.
- Bolio, E. J., Yasuna, J. A. & Sinclair, J. L. 1995 Dilute turbulent gas-solid flow in risers with particle-particle interactions. *AIChE Journal* 41, 1375–1388.
- Botto, L., Narayanan, C., Fulgosi, M. & Lakehal, D. 2005 Effect of nearwall turbulence enhancement on the mechanisms of particle deposition. *Int. J. Multiphase Flow* $\bf 31$, 940–956.
- CARAMAN, N., BOREE, J. & SIMONIN, O. 2003 Effect of collisions on the dispersed phase fluctuation in a dilute tube flow: Experimental and theoretical analysis. *Phys. Fluids* **15**, 3602–3612.
- CERBELLI, S., GIUSTI, A. & SOLDATI, A. 2001 ADE approach to predicting dispersion of heavy particles in wall-bounded turbulence. *Int. J. Multiphase Flow* 27, 1861–1879.
- Chan, C. K., Guo, Y. C. & Lau, K. S. 2005 Numerical modeling of gas-particle

- flow using a comprehensive kinetic theory with turbulence modulation. *Powder Technology* **150**, 42-55.
- Crowe, C., Sommerfeld, M. & Tsuji, Y. 1998 Multiphase flows with droplets and particles. CRC Press.
- DAVIS, T. 2004 Algoritm 832: Umfpack, an unsymmetric-pattern multifrontal method. ACM Transactions on Mathematical Software 30, 196–199.
- Do-Quang, M., Villanueva, W., Amberg, G. & Loginova, I. 2007 Parallel adaptive computation of some time-dependent materials-related microstructural problems. *Bulletin of the Polish Academy of Sciences* 55, 229–237.
- Elghobashi, S. 1994 On predicting particle-laden turbulent flows. Applied Scientific Research 52, 309–329.
- Elghobashi, S. E. & Abou-Arab, T. W. 1983 A two-equation turbulence model for two-phase flows. *Phys. Fluids* **26**, 931–938.
- ENWALD, H., PEIRANO, E. & ALMSTEDT, A.-E. 1996 Eulerian two-phase flow theory applied to fluidization. *Int. J. Multiphase Flow* 22, 21–66.
- FAN, L.-S. & Zhu, C. 1998 Principles of gas-solid flows. Cambridge University Press.
- Fessler, J. R., Kulick, J. D. & Eaton, J. K. 1994 Preferential concentration of heavy particles in a turbulent channel flow. *Phys. Fluids* **6**, 3742–3749.
- Fevrier, P., Simonin, O. & Squires, K. D. 2005 Partitioning of particle velocities in gas-solid turbulent flows into a continuous field and a spatially uncorrelated random distribution: theoretical formalism and numerical study. *J. Fluid Mech.* 533, 1–46.
- FRIEDLANDER, S. & JOHNSTONE, H. 1957 Deposition of suspended particles from turbulent gas streams. *Ind. and Eng. Chem.* **49**, 1151–1156.
- GORE, R. & CROWE, C. 1991 Modulation of turbulence by a dispersed phase. Trans. of ASME J. Fluids Engn. 113, 304–307.
- Guermond, J.-L. & Quartapelle, L. 1997 Calculation of incompressible viscous flows by an unconditionally stable projection FEM. *Journal of Computational Physics* 132, 12–33.
- Gullman-Strand, J., Amberg, G. & Johansson, A. V. 2004 Turbulence and scalar flux modelling applied to separated flows. *Tech. Rep.* Department of Mechanics, Royal Institute of Technology, Stockholm Sweden.
- HAARLEM, B., BOERSMA, B. & NIEUWSTADT, F. 1998 Direct numerical simulation of particle deposition onto a free-slip and no-slip surface. *Phys. Fluids* 10, 2608– 2620.
- HADINOTO, K. & CURTIS, J. S. 2004 Effect of interstitial fluid on particle-particle interactions in kinetic theory approach of dilute turbulent fluid-particle flow. Ind. Eng. Chem. Res. 43, 3604–3615.
- Hetsroni, G. 1989 Particles-turbulence interaction. Int. J. of Multiphase Flow. 15, 735–746.
- HINZE, J. O. 1959 Turbulence. McGraw-Hill book company.
- Ishii, M. 1975 Thermo-Fluid Dynamic Theory of Two-Phase Flow. Eyrolles, Paris.
- Jenkins, J. & Richman, M. 1985 Grad's 13-moment system for a dense gas of inelastic spheres. *Archive for rational mechanics and analysis* 87, 355–377.
- JOHANSEN, S. 1991 The deposition of particles on vertical walls. Int. J. Multiphase Flow 17, 355–376.

- JOHNSON, P. C. & JACKSON, R. 1987 Frictional-collisional constitutive relations for granular materials with application to plane shearing. J. Fluid Mech. 176, 67–93.
- Kanther, W., Grüner, C., Götz, S. & Strauss, K. 2003 Coupling of deterministic and stochstic simulation methods for gas-solid flows. *Proc. Aool. Math. Mech.* **3**, 408–411.
- Kuipers, J., van Duin, K., van Beckum, F. & van Swaaij, W. 1992 A numerical model of gas-fluidized beds. *Chem. Eng. Sci.* 35, 1913–1924.
- Kulick, J. D., Fessler, J. R. & Eaton, J. K. 1994 Particle response and turbulence modification in fully developed channel flow. J. Fluid Mech. 277, 109–134.
- LI, Y., MCLAUGHLIN, J., KONTOMARIS, K. & PORTELA, L. 2001 Numerical simulation of particle-laden turbulent channel flow. Phys. Fluids 13, 2957–2967.
- LIU, B. Y. H. & AGARWAL, J. 1974 Experimental observation of aerosol deposition in turbulent flow. Aerosol Science 5, 145–155.
- LJUS, C., JOHANSSON, B. & ALMSTEDT, A.-E. 2002 Turbulence modification by particles in a horizontal pipe flow. *Int. J. of Multiphase Flow.* **28**, 1075–1090.
- LOTH, E. 2000 Numerical approaches for motion of dispersed particles, droplets and bubbles. *Progr. Energy and Comb. Sci.* **26**, 161–223.
- Louge, M. Y., Mastorakos, E. & Jenkins, J. K. 1991 The role of particle collisions in pneumatic transport. *J. Fluid Mech.* **231**, 345–359.
- Lun, C. K. K. & Liu, H. S. 1997 Numerical simulation of dilute turbulent gas-solid flows in horizontal channels. *Int. J. Multiphase Flow* **23**, 575–605.
- Lun, C. K. & Savage, S. B. 2003 Lecture notes in physics: Granular Gas Dynamics Kinetic theory for inertia flows of dilute turbulent gas-solid mixtures. Springer.
- Lun, C. K. K., Savage, S. B., Jeffrey, D. J. & Chepurniy, N. 1984 Kinetic theories for granular flow: inelastic particles in couette flow and slightly inelastic particle in a general flow field. *J. Fluid Mech.* 140, 223–256.
- Mashayek, F. & Pandya, R. 2003 Analytical description of particle/droplet-laden turbulent flows. *Progr. Energ. and Comb. Sc.* **29**, 329–378.
- MAXEY, M. R. & RILEY, J. J. 1983 Equations of motion for a small rigid sphere in a nonuniform flow. *Phys. Fluids* **26**, 883–889.
- MELVILLE, W. & Bray, K. 1979 A model of the two-phase turbulent jet. Int. J. Heat Mass Transfer 22, 647–656.
- MITO, Y. & HANRATTY, T. 2006 Effect of feedback and inter-particle collisions in an idealized gas-liquid annular flow. Int. J. Multiphase Flow 32, 692–716.
- MITTER, A., MALHOTRA, J. & JADEJA, H. 2004 The two fluid modelling of gasparticle transport phenomenon in confined systems considering inter particle collision effects. *Int. J. Numer. Meth. Heat & Fluid Flow* 14, 579–605.
- NARAYANAN, C., LAKEHAL, D., BOTTO, L. & SOLDATI, A. 2003 Mechanisms of particle deposition in a fully developed turbulent open channel flow. *Phys. Fluids* 15, 763–775.
- NASR, H., AHMADI, G. & McLauglin, J. 2009 A DNS study of effects of particleparticle collisions and two-way coupling on particle deposition and phasic fluctuations. J. Fluid Mech. 640, 507–536.
- Peirano, E. & Leckner, B. 1998 Fundamentals of turbulent gas-solid flows applied to circulating fluidized bed combustion. *Prog. Energy Combust. Sci.* 24, 259–296.

- POURAHMADI, F. & HUMPHREY, J. 1983 Modeling solid-fluid turbulent flows with application to predicting erosive wear. *PCH Physico Hydrodynamics* 4, 191–219.
- REEKS, M. 1983 The transport of discrete particles in inhomogeneous turbulence. *J. Aerosol Sci.* 14, 729–739.
- REEKS, M. 1993 On the constitutive relations for dispersed particles in nonuniform flows. I: Dispersion in a simple shear flow. *Phys. Fluids A* 5, 750–761.
- REEKS, M. W. 1977 On the dispersion of small particles suspended in an isotropic turbulent fluid. *J. Fluid Mech.* **83**, 529–546.
- Reeks, M. W. 1991 On a kinetic equation for the transport of particles in turbulent flows. *Phys. Fluids A* 3, 446–456.
- ROUSON, D. & EATON, J. 2001 On the preferential concentration of solid particles in turbulent channel flow. J. Fluid Mech. 428, 149–169.
- SAFFMAN, P. G. 1965 The lift of a small sphere in a shear flow. *J. Fluid Mech* 22, 385–400.
- SAFFMAN, P. G. 1968 Corrigendum to the lift of a small sphere in a shear flow. J. Fluid Mech 31, 624—.
- Schuller, L. & Naumann, A. 1933 Über die grundlegenden Berechnungen bei der Schwerkraftaufbereitung. Ver. Deut. Ing. 77, 318–320.
- Shin, M., Kim, D. & Lee, J. 2003 Deposition of inertia-dominated particles inside a turbulent boundary layer. *Int. J. Multiphase Flow* **29**, 893–926.
- Simonin, O., Deutsch, E. & Minier, J. 1993 Eulerian prediction of the fluid/particle correlated motion in turbulent two-phase flows. *Applied Scientific Research* **51**, 275–283.
- Sinclair, J. & Jackson, R. 1989 Gas-particle flow in a vertical pipe with particle-particle interactions. $AIChE\ J.\ 35,\ 1473-1486.$
- SLATER, S., LEEMING, A. & YOUNG, J. 2003 Particle deposition from twodimensional turbulent gas flows. Int. J. Multiphase Flow 29, 721–750.
- SOLDATI, A. & MARCHIOLI, C. 2009 Physics and modelling of turbulent particle deposition and entrainment: Review of a systematic study. *Int. J. Multiphase Flow* 35, 827–839.
- Sommerfeld, M. 1992 Modelling of particle-wall collisions in confined gas-particle flows. *Int. J. Multiphase Flow* 18, 905–926.
- Sommerfeld, M. 2000 Theoretical and experimental modelling of particulate flows. Lecture Series, von Karman Institute of Fluid Dynamics part I and II, 1–63.
- Sommerfeld, M. 2003 Analysis of collision effects for turbulent gas-particle flow in a horizontal channel: Part I. particle transport. *Int. J. Multiphase Flow* **29**, 675–699.
- Sommerfeld, M., van Wachem, B. & Oliemans, R. 2007 Dispersed turbulent multi-phase flow. Best practice guidelines.. ERCOFTAC.
- SQUIRES, K. & EATON, J. 1991 Measurement of particle dispersion obtained from direct numerical simulations of isotropic turbulence. J. Fluid Mech. 226, 1–35.
- Strömgren, T., Brethouwer, G., Amberg, G. & Johansson, A. V. 2008 Model simulations of two-way coupling effects on eveolving particle-laden turbulent channel flow. Proceedings of the 7th Int. Symposium on Engineering Turbulence Modelling and Measurements. Limassol, 2008, Editors: M.A. Leschziner, S. Kassinos pp. 480–485.

- Strömgren, T., Brethouwer, G., Amberg, G. & Johansson, A. V. 2009a Modelling of turbulent gas-particle flows with focus on two-way coupling effects on turbophoresis. Submitted to Int. J. Multiphase Flow pp. –.
- Strömgren, T., Brethouwer, G., Amberg, G. & Johansson, A. V. 2009b A study of particle feedback in turbulent gas-particle flows. 7th World Conference on Experimental Heat Transfer, Fluid Mechanics and Thermodynamics. Krakow, July 2009, Editors: J.S. Szymd, J. Spałek, T.A. Kowalewski pp. 1633–1640.
- Tanaka, T. & Tsuji, Y. 1991 Numerical simulation of gas-solid two-phase in a vertical pipe: on the effect of inter-particle collision. 4th Symposium on Gas-Solid Flows, ASME FED 121, 123–128.
- Taulbee, D. B., Mashayek, F. & Barré, C. 1999 Simulation and reynolds stress modeling of particle-laden turbulent shear flows. *Int. J. Heat and Fluid Flow* 20, 368–373.
- Thai Van, D., Minier, J. P., Simonin, O., Freydier, P. & Olive, J. 1994 Multidimensional two-fluid model computation of turbulent dispersed two-phase flows. *Numerical methods for multiphase flows, ASME* 185, –.
- Tsuji, Y., Morikawa, Y. & Shiomi, H. 1984 LDV measurements of an air-solid two-phase flow in a vertical pipe. *J. Fluid Mech.* **139**, 417–434.
- Tu, J. & Fletcher, C. 1994 An improved model for particulate turbulence modulation in confined two-phase flows. *Int. Comm. Heat and Mass Transfer* 21, 775–783.
- Vance, M., Squires, K. & Simonin, O. 2006 Properties of the particle velocity field in gas-solid turbulent channel flow. *Phys. Fluids* 18, 063302.
- VREMAN, A. 2007 Turbulence characteristics of particle-laden pipe flow. *J. Fluid Mech.* **584**, 235–279.
- WALLIN, S. & JOHANSSON, A. 2000 An explixit algebraic Reynolds stress model for incompressible and compressible turbulent flows. J. Fluid Mech. 403, 89–132.
- Wang, Q. & Squires, K. 1996 Large eddy simulation of particle deposition in a vertical turbulent channel flow. *Int. J. Multiphase Flow* 22, 667–683.
- Wang, Y., Komori, S. & Chung, M. K. 1997 A two-fluid turbulence model for gas-solid two-phase flows. *J. Chem. Eng. Japan* **30**, 526–534.
- Wells, M. & Stock, D. 1983 The effects of crossing trajectories on the dispersion of particles in a turbulent flow. *J. Fluid Mech.* **136**, 31–62.
- Wood, A. M., Hwang, W. & Eaton, J. K. 2005 Preferential concentration of particles in homogeneous and isotropic turbulence. *Int. J. Multiphase Flow* 31, 1220–1230.
- Yamamoto, T., Potthoff, M., Tanaka, T., Kajishima, T. & Tsuji, Y. 2001 Large-eddy simulation of turbulent gas-particle flow in a vertical channel: effect of considering inter-particle collisions. *J. Fluid Mech.* 442, 303–334.
- Yarin, L. P. & Hetsroni, G. 1994 Turbulence intensity in dilute two-phase flows

 III; the particles-turbulence interaction in dilute two-phase flow. Int. J. of Multiphase Flow. 20, 27–44.
- Young, J. & Leeming, A. 1997 A theory of particle deposition in turbulent pipe flow. J. Fluid Mech. 340, 129–159.
- Yuan, Z. & Michaelides, E. 1992 Turbulence modulation in particulate flows A theoretical approach. *Int. J. Multiphase Flow* 18, 779–785.

- ZAICHIK, L. 1999 A statistical model of particle transport and heat transfer in turbulent shear flows. *Phys. Fluids* 11, 1521–1534.
- Zhang, D. & Rauenzahn, R. 1997 A viscoelastic model for dense granular flows. J. Rheol. 41, 1275–1298.
- Zhang, Y. & Reese, J. M. 2003 Gas turbulence modulation in a two-fluid model for gas-solid flows. $AIChE\ Journal\ 49,\ 3048-3065.$
- Zhou, L. X. 2010 Advances in studies on two-phase turbulence in dispersed multiphase flows. *Int. J. Multiphase Flow* **36**, 100–108.
- Zhou, L. X. & Chen, T. 2001 Simulation of swirling gas-particle flows using usm and $k-\epsilon-kp$ two-phase turbulence models. *Powder Technology* **114**, 1–11.